Exhumation and Paleo-Heat Flow of the Shimanto Accretionary Complex, Shikoku, Southwest Japan

-Vitrinite Reflectance and Fluid Inclusion Study-

Arito SAKAGUCHI

A dissertation submitted
to the Doctoral Program in Geoscience,
University of Tsukuba
in partial fulfillment of the requirements
for the degree of Doctor of Philosphy (Science)

January, 1997

CONTENTS

LIST OF TABLES

page

LIST OF FIGURES

page

ABSTRACT

The P-T condition in the Shimanto accretionary complex, southwest Japan was determined by combining the vitrinite reflectance with homogenization temperature of the fluid inclusion analysis. Low grade metamorphism was discussed concerning the accretionary complex development. This is the first report on the quantitive P-T path in the accretionary complex.

The Cretaceous Shimanto accretionary complex is separated from the Jurassic Chichibu accretionary complex on the north by the Butsuzo Tectonic Line (BTL) and is separated from the Tertiary Shimanto accretionary complex on the south by the Aki Tectonic Line (ATL). The complex is composed mostly of trench-fill sediments, slope-basin sediments and melanges. The age difference between the oceanic rock blocks and black shale matrix in the melange decreases southward from the Jurassic to Tertiary complex. This trend implies that a spreading ridge approached to the trench during accretionary complex formation. Mid-oceanic-ridge basalt (MORB)-type blocks are thought to be uncommon in most of the melanges in Japan, but the youngest melange in the Cretaceous Shimanto Belt is characterized by presence of MORB-type basalt blocks without pelagic sediment.

Vitrinite reflectance is a responsive indicator for the thermal

diagenesis, and the fluid inclusion within the vein mineral preserves the same conditions of the volume and density at trapping. The isochore that is the internal P-T growth line within the fluid inclusion is obtained from the homogenization temperature by heating experiment. The intersection of the maximum temperature and the isochore indicates the maximum pressure limit of the fluid. The pressure of the each stage of the methane-rich and water-rich fluid trapping are estimated by this P-T intersection and then the paleo-geothermal gradient is obtained from two different samples from the same geologic unit.

The thermal structural analysis of the Chichibu and Shimanto accretionary complex in the western Shikoku Island by the vitrinite reflectance indicated that the thermal structure is independent of the geologic structure. The repeated southward increase trend of thermal structure penetrates all the formations and melanges even the shelf sediments. This indicates that the complexes suffered thermal overprint after accretion.

It was revealed by the present study that the fluid of methane and water separately migrated at different P-T stages during metamorphism. Judging from the mode of occurrence of the vein minerals and correlation of the homogenization temperature of the water-rich fluid inclusion with the vitrinite reflectance, the water-rich

fluid was trapped at later stage than the methane-rich fluid. The methane-rich fluid was trapped into quartz vein mineral under higher pressure of ~260 MPa with lower geothermal gradient of ~24 °C/km at the early stage than the water-rich fluid of ~125 MPa with the higher geothermal gradient of 50~ °C/km at the later stage. This late stage geothermal gradient increases trenchward, and it becomes over 90 °C/km in the Okitsu Melange.

The Okitsu Melange suffered much higher temperature than the surrounding strata, and was considered to be formed concurrently with the Kula-Pacific ridge subduction with remarkable formation of many small quartz veins. The high heat might be transferred by fluid migration in the toe of the accretionary prism. This event occurred as the thermal overprint in the late stage.

The paleo-heat flow estimated from the P-T conditions is consistent with the heat flow estimated from the age of the slab for the two stages. The results suggest that the heating by the slab is definitely effective for the metamorphism in the accretionary prism even by cold plate subduction. In conclusion, the metamorphism in the Shimanto accretionary complex was evolved with the change of the thermal condition of the slab, and both fluids of methane and water recorded the P-T conditions during accretion and later thermal event, respectively.

Chapter 1

INTRODUCTION

I succeeded in determining the P-T conditions of various place in the Cretaceous Shimanto accretionary complex in the western Shikoku Island, southwest Japan by using the vitrinite reflectance and the homogenization temperature of the fluid inclusion within the quartz and calcite veins. Furthermore, I could discuss the paleo-heat flow and quantity of uplift of the complex obtaining different P-T conditions from the differnt place within the same unit of the complex. Two stgaes of fluid inclusions were also inferred from different vein generation, and the P-Tconditions and their tectonic implications, one for the early, the other for the late stage were also discussed. This is the first study of the P-T path in the accretionary complex.

Although the structural analysis of melange (Hsu, 1968; Moor and Wheeler, 1978; Cowan, 1985; Kimura and Mukai, 1991 etc.), thermal structural modeling by simulation (Dumitru et al., 1985) and metamorphic facies analysis of the exotic blocks (Cowan, 1974; Sample and Moor, 1987; Toriumi and Teruya, 1988) have been investigated in accretionary complex in various areas, the P-T path was no more than speculation. Vrolijk (1987; 1988) discussed the thermal effect by warm fluid migration within the Kodiak accretionary prism toe based on the methane-rich fluid inclusion study. However, it is not clear the thermal structure and its tectonic significance.

Over a last few years, a considerable number of studies have been made on estimation of the maximum temperature of the accretionary complex by the vitrinite reflectance and illite crystallinity, and it is known that the Shimanto accretionary complex underwent high temperature (Aihara et al., 1987; Mori and Taguchi, 1988; DiTullio et al., 1993). Sakaguchi et al. (1992, 1994, 1996), Underwood et al. (1992, 1993) and Hibbard et al. (1993) pointed out that the Shimanto accretionary complex has suffered thermal overprint by the young plate subduction. However, these discussions have some difficult problems that the maximum temperature includes various factors such as burial depth, change of geothermal gradient and thermal effect of igneous activity.

The fluid expulsion in the present Nankai accretionary prism is well known, and its tectonic context was discussed (Chamot-Rooke et al., 1992). Although the heat transfer to the toe of the accretionary prism by the fluid was suggested from the heat flow distribution also in the Nankai accretionary prism (Ashi and Taira 1993), little is known about the circumstance of the fluid flow in the ancient Shimanto accretionary complex on land.

The data of the P-T condition during fluid trapping within vein mineral offer the key to understanding these subjects. In this thesis, each fluid of methane and water was found within the vein minerals, and it was revealed that they were to be trapped at different stages during metamorphism. Then becomes possible to know the thermal evolution and fluid migration at those times. As a result, the P-T path, paleo-heat flow distribution and their relation

with fluid migration in the Shimanto accretionary complex were obtained for a case study in the western Shikoku Island, and it was proposed that the metamorphism of the accretionary complex is dominantly controlled by the thermal condition of the subducting plate.

Chapter 2

GEOLOGIC SETTING

The Cretaceous Shimanto accretionary complex is separated from the Jurassic Chichibu accretionary complex on the north by the Butsuzo Tectonic Line (BTL) and is separated from the Tertiary Shimanto accretionary complex on the south by the Aki Tectonic Line (ATL).

The Cretaceous Shimanto accretionary complex is composed of two groups, the lower Cretaceous Shinjogawa and upper Cretaceous Taisho Groups. The Tertiary Shimanto accretionary complex is composed of two groups; the Eocene to lower Oligocene Hata and upper Oligocene to lower Miocene Nabae Groups. There is a sedimentary age difference of several tens of million of years between these groups.

The most part of the complex consistents of dominant sediment of the trench-fill facies, however three units of melange facies of the Yokonami, Kure and Okitsu Melanges are interleaved within the Taisho Group in the Cretaceous complex (Taira et al., 1980). Moreover, the shelf and forearc facies overlie these complexes unconformably; they are the Cretaceous Monobegawa Group and Torinosu Group on the Chichibu accretionary complex, Doganaro Formation, Uwagumi Formation and Uwajima Group on the Shinjogawa Group, and the Miocene Misaki Group on the Nabae Group (Okamura, 1992; Morino, 1993; Kimura, 1985) (Fig. 1.)

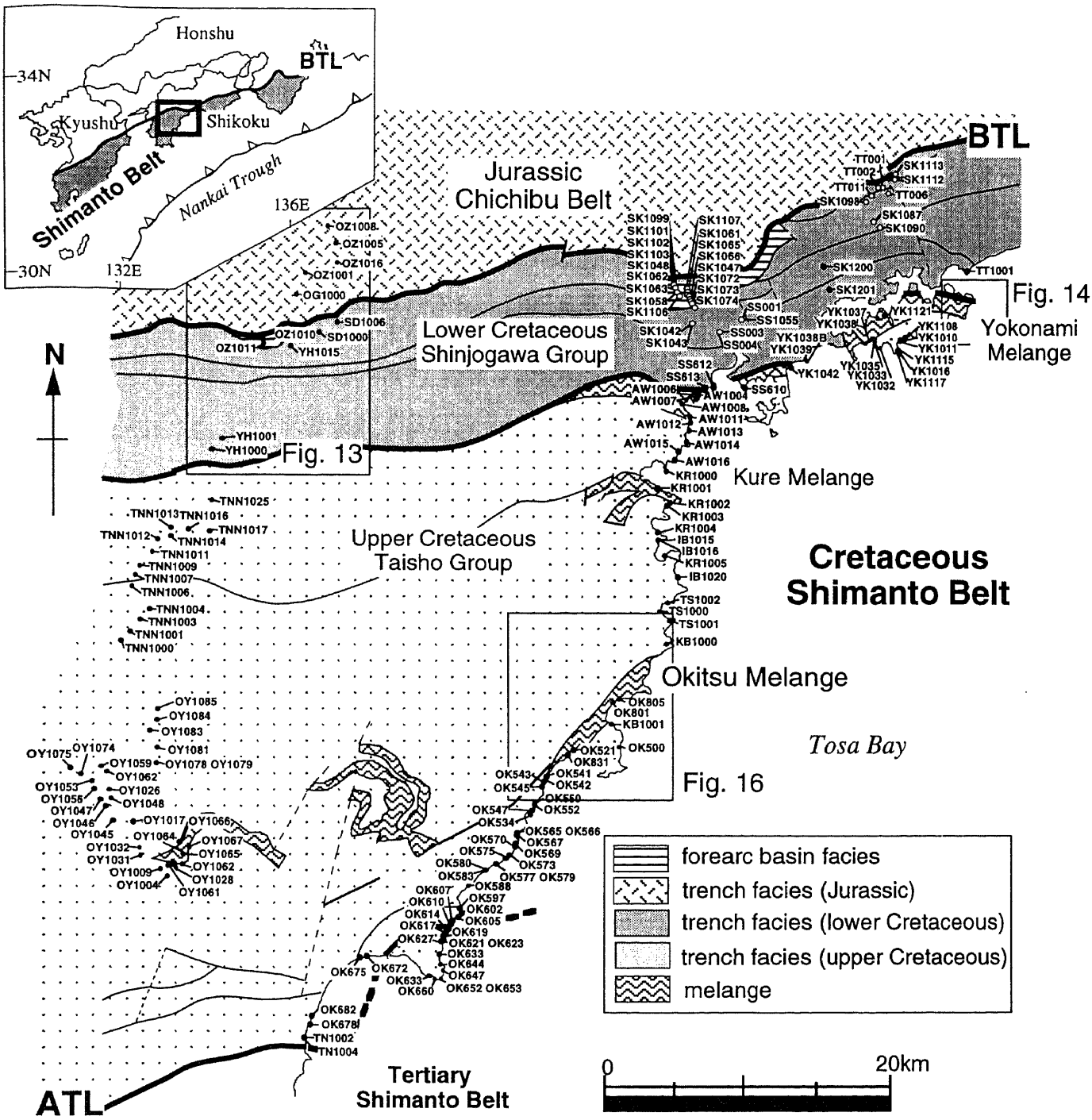

Figure 1. Schematic geologic map and sampling points of the vitrnite in the Cretaceous Shimanto accretionary complex. The schematic geologic map in the Cretaceous Shimanto accretionary complex, western Shikoku. The Cretaceous unit is divided from the Jurassic unit by the Butsuzo tectonic line (BTL) and divided from the Tertiary unit by the Aki tectonic line (ATL). The Cretaceous unit is composed of two Groups of lower Cretaceous Shinjogawa and upper Cretaceous Taisho. Two hundreds of vitrinite were sampled from all the formations and melanges along the coastal area of Tosa bay and Shimanto river system area. The vitrinite reflectance data of open circles are from Ohmori (1994).

The sediments of the trench-fill, forearc and shelf facies have coherent turbidite sequence and tightly folded structure. In contrast, the melange facies suffered strong deformation and includes exotic oceanic crustal blocks. The age difference between the oceanic rock blocks and black shale matrix in the melange decreases southward from Jurassic to Tertiary complex (Taira et al., 1988). This trend may imply that a spreading ridge had approached to the trench. Mid-oceanic-ridge basalt (MORB)-type blocks are uncommon in most of the melanges in Japan (Ogawa and Taniguchi, 1989; Sakamoto et al., 1993), but the youngest melange in the Cretaceous Shimanto Belt is characterized by presence of MORB-type basalt blocks without pelagic sediment (Kiminami and Miyashita, 1992; Kiminami et al., 1992).

In the southernmost portion of the Tertiary complex, the Ashizuri Granite intruded into the Shimizu Formation at 14 m. y. B. P. (Shibata and Nozawa, 1968; Takahashi, 1980)(Fig. 2), and gave contact metamorphism to the surrounding strata.

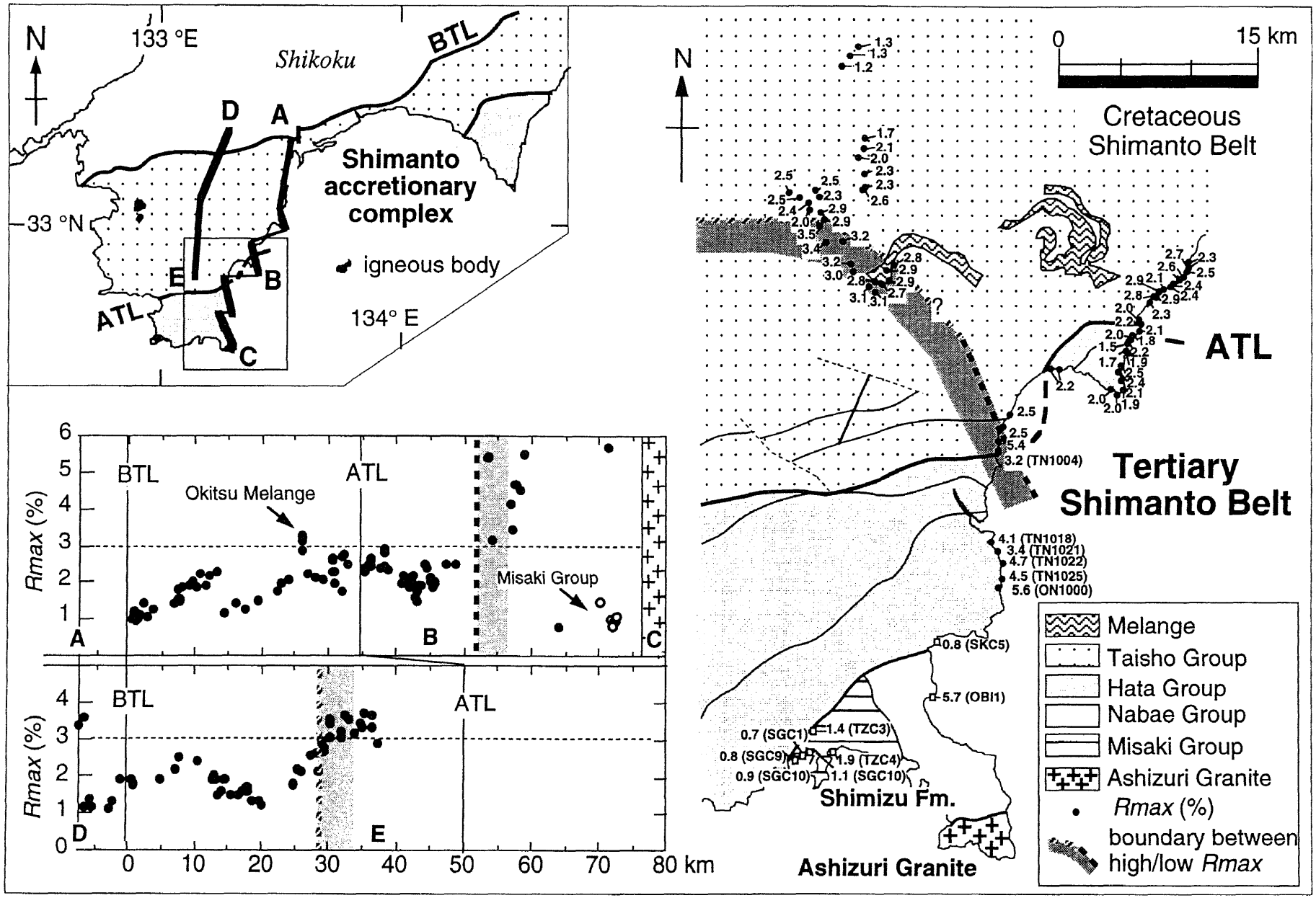

Figure 2. Sampling points of the vitrnite in the Tertiary unit and high vitrinite reflectance region.The Geologic map of the southernmost portion in the Shimanto accretionary complex. The Ashizuri Granite, intruded at middle Miocene, caused contact metamorphosis to surrounding strata. The region within 20-50 km around Ashizuri Granite has much higher vitrinite reflectance than the northern area. The vitrinite reflectance data of open squares are from Okano (1992).

Chapter 3

METHODS

3.1 Vitrinite reflectance analysis

Two hundred of coals for vitrinite reflectance analysis were sampled in the western coastal area of the Tosa Bay and the inland area along the Shimanto River system (Figs. 1 and 2). I picked up the coal concentrated layer and coal fragment from the both sandstone and black shale (Figs. 3a and 3b). The coal fragments are interleaved with clastic grains (Figs. 3c and 3d).

The vitrinites were sampled from all the facies, concentrating in the significant areas such as around the BTL, Yokonami Melange and Okitsu Melange. In the case of the Yokonami Melange, the vitrinites were sampled both from the sandstone block and black shale matrix.

Vitrinite reflectance is a responsive indicator for the thermal diagenesis. The reflectance measurement was carried out in accordance with the Japanese Industrial Standard, using the Leitze Ortholux microscope equipped with a photomultiplier. The diagram of the measuring device is shown in Figure 4. I calibrated the reflectance by the standard of the Berry and Associate Company under the green light (546 nm.) (Fig. 4). I discriminated between the vitrinite and the other macerals under the microscope (Fig. 3d).

For each sample, a hundred of the vitrinite particles were measured on

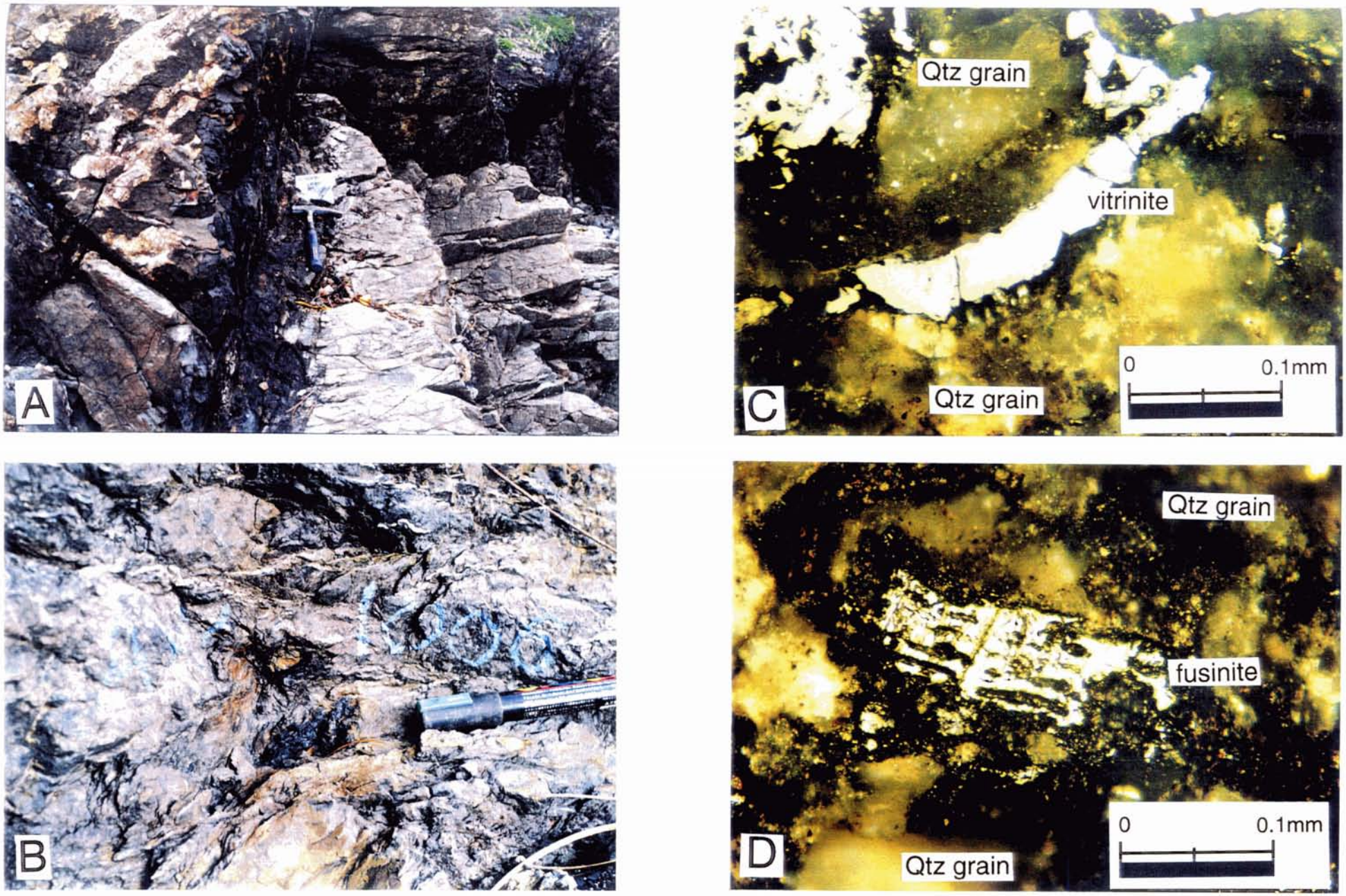

Figure 3. Occurence of the vitrinite. The vitrinite was sampled from the coal concentrated layer and coal fragment from the both sandstone and black shale.

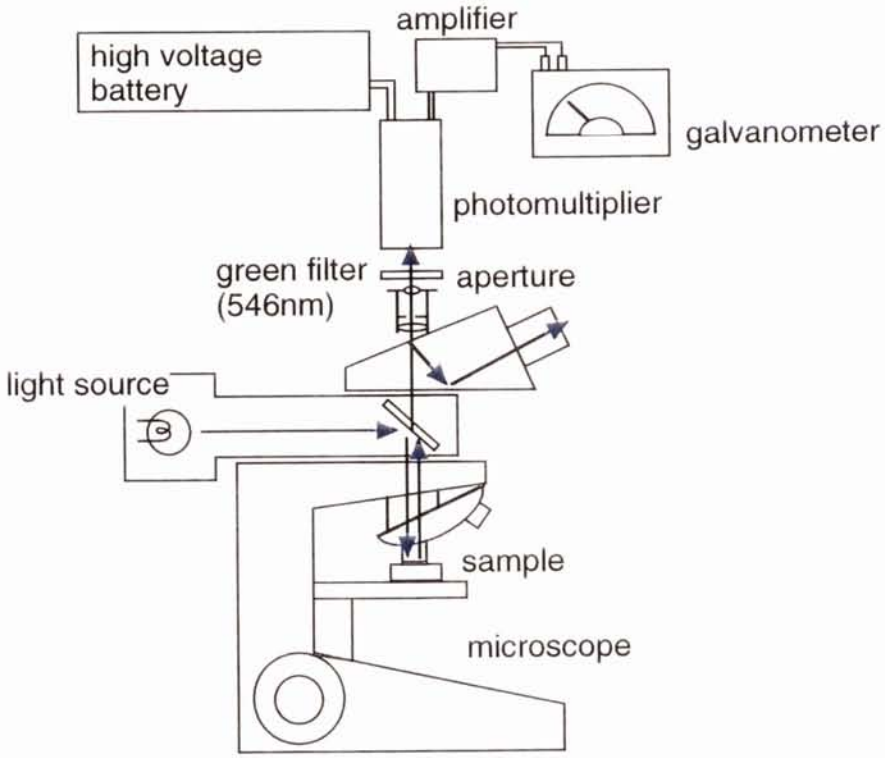

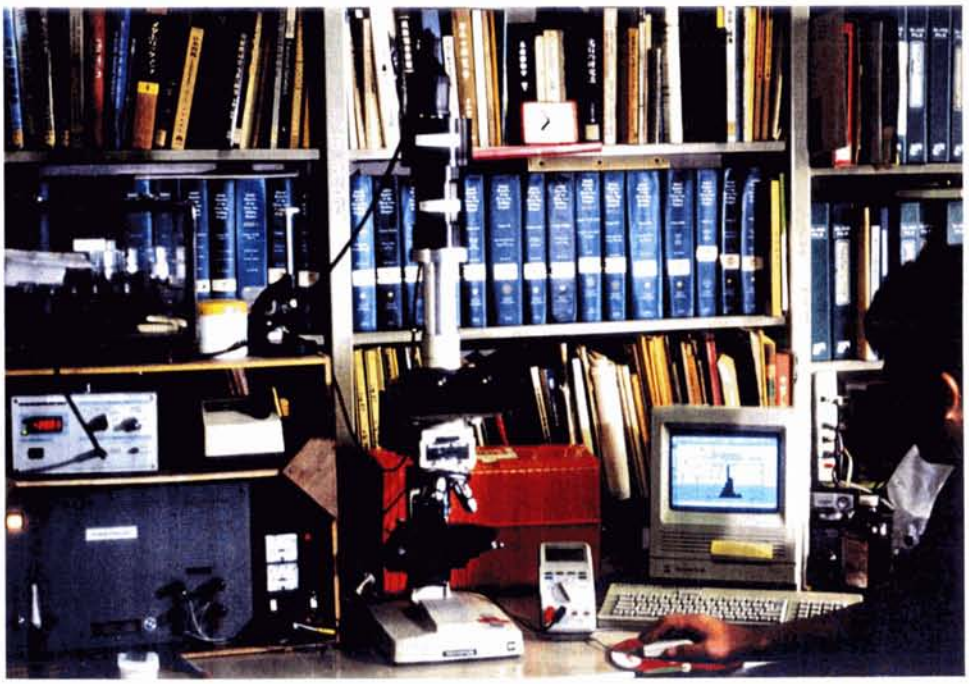

Figure 4. Diagram of the measuring device and appearence for vitrinite reflectance. The vitrinite reflectance was measured by the photomultiplier with green light of 546 nm in wave length.

three types reflectances of random mean (Rm), maximum (Rmax) and minimum reflectance (Rmin) during the rotation of the stage under the polarizing-microscope. Although the Rmax is a true reflectance for maturation vitrinite, the most of studies for the maximum temperature estimation used the Rm, is obtained on the stage with fixed position. Therefore, I use the Rmax for analysis of thermal structure and the Rm for the estimating the maximum temperature.

Barker's (1988) method for estimating the maximum temperature is accurate for samples from the Shimanto accretionary complex (Laughland and Underwood, 1993). I estimated the maximum temperature from the mean vitrinite reflectance according to the equation of T (°C) = 148 + (104 [ln %Rm]) with the error of ± 30 °C.

3.2 Fluid inclusion analysis

Twenty-five quartz and calcite veins are sampled with the same outcrop of the vitrinite from the three of the turbidite units and two of melange units; such as Susaki Formation, Shimotsui Formation, Nonokawa Formation for the former units, Yokonami Melange and Okitsu Melange for the latter units. The veins that is composed many of small veins are parallel or sub-parallel with the layer (Fig. 5a). They are complicated, and it is not easy to identify the

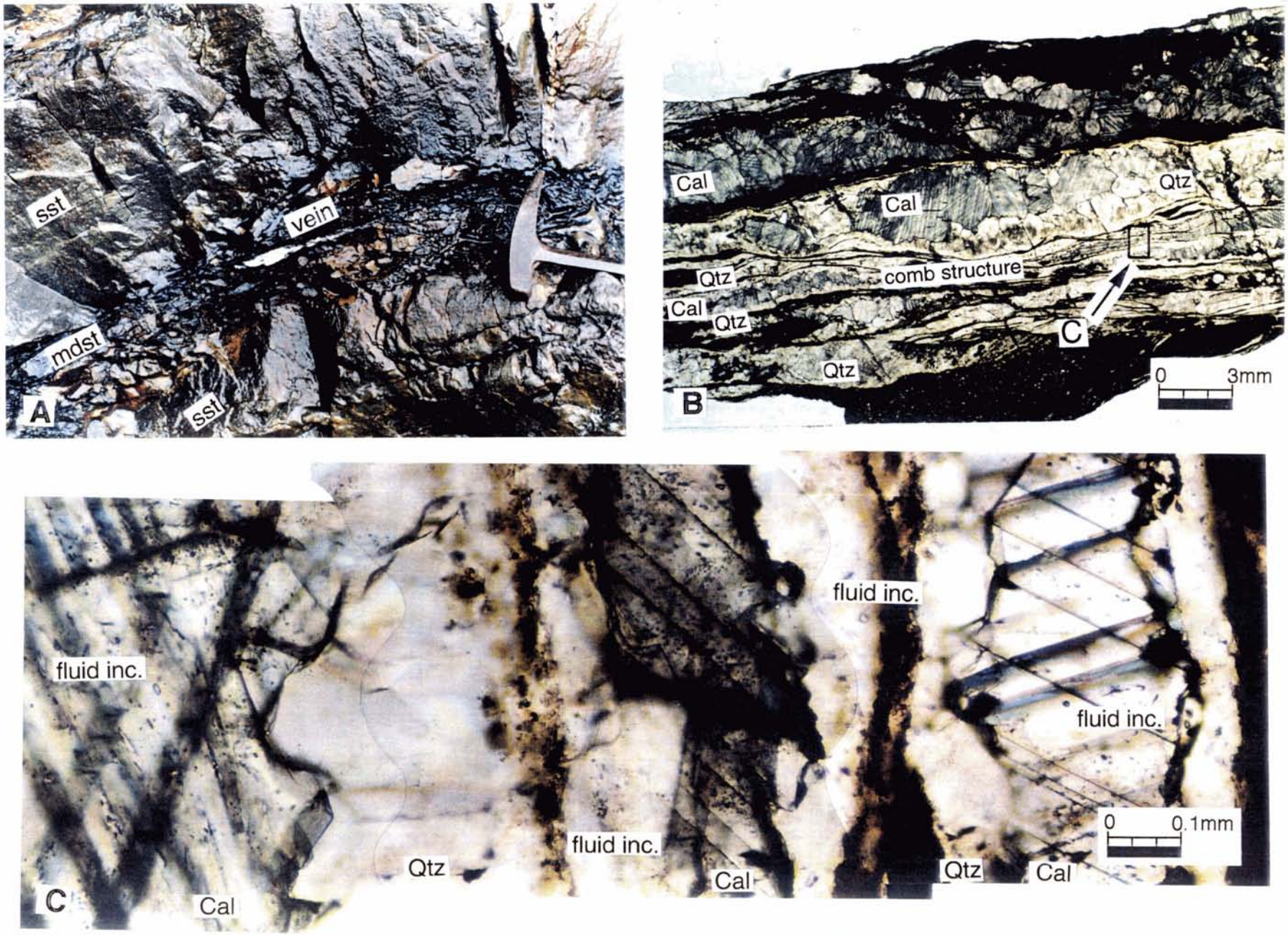

Figure 5. Occurence of the veine mineral. The veine, paralell or subparalell with the layer was sampled. The one veine is coposed of many small veines. It is difficult to identify the formation order of each vein

formation order of each vein. However, it is known that a quartz was deposited earlier than calcite, because the quartz crystals tend to be euhedral with the comb structure, and the calcite crystal tends to be anhedral.

The fluid inclusions within the double polished rock wafer were experimented by the heating and cooling stage of the Linkam THM-600 (Fig. 6) with the error of 5 °C. The device was calibrated by the melting temperature of the Dyphenylamine (54 °C), Phenolphthalein (262 °C) and Potassium Dichromate (396 °C.)

The two types fluid inclusions are observed; the one is of one phase and the other is of phases of liquid and vapor fluid inclusions in the room temperature (Fig. 7a). In general, the one phase fluid inclusion occurs within the quartz veins and darker than the other, and is divided into two phases in the cooling experiment lower than -100 °C (Fig. 7c and 7d). The phases differ in composition; the early type is water rich and the later type is methane-rich. The detail discussion about the fluid composition is shown later.

The liquid and vapor within the fluid inclusion are homogenized by heating. Internal pressure of the fluid inclusion increases along the isochore after homogenization (Fig. 8). The P-T condition during fluid trapping plots somewhere along the isochore, and the intersection of the isochore and maximum temperature indicates the upper limit of the pressure condition for the fluid. The geothermal gradient during fluid trapping is estimated from the difference of the P-T condition between the sea floor and fluid. I used the

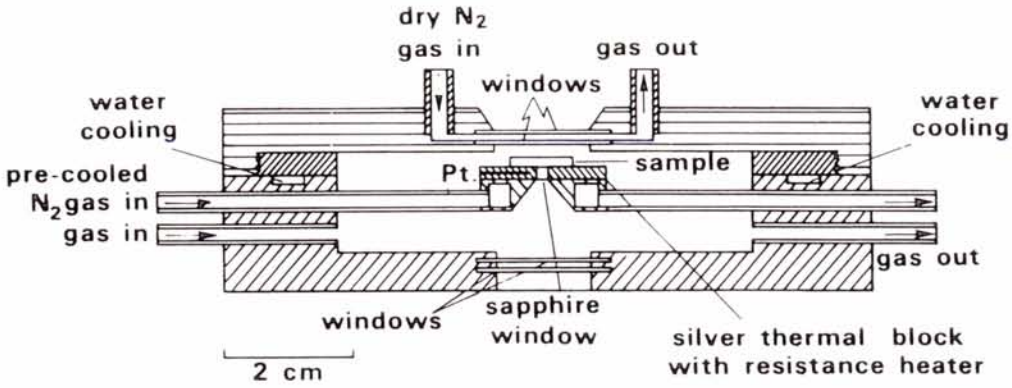

Shepherd (1981)

Figure 6. Diagram of the heating stage and appearence. The fluid inclusions were experimented by the heating and cooling stage of the Linkam THM-600 with the error of 5 °C.

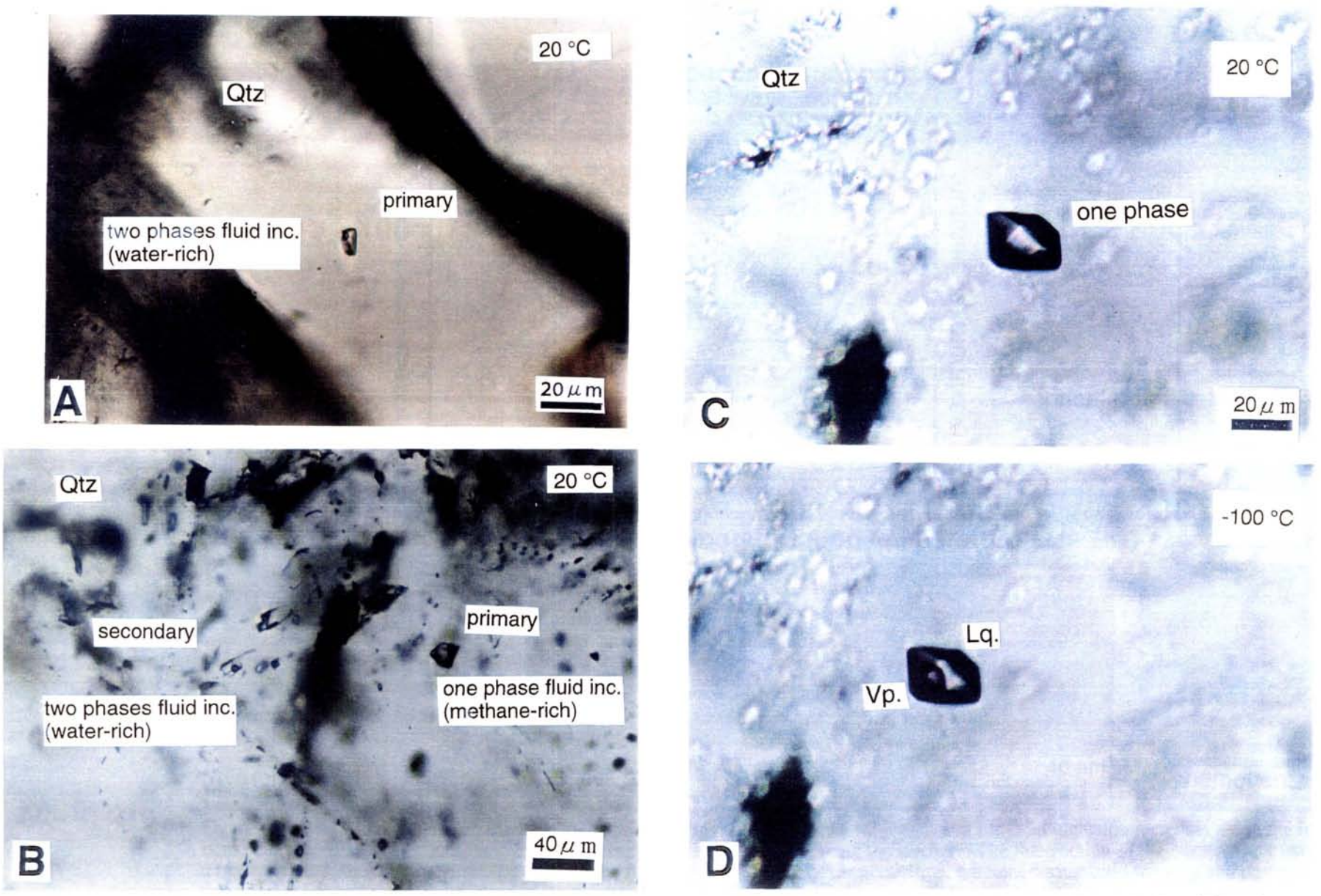

Figure 7. Water-rich fluid inclusion and methane-rich fluid inclusion. The two types fluid inclusions are observed; such as one phase (B, C and D) and two phases (A) of liquid and vapor fluid inclusions in the room temperature. The fluid of this type is divided into two phases by the cooling experiment lower than -100 °C (C and D).

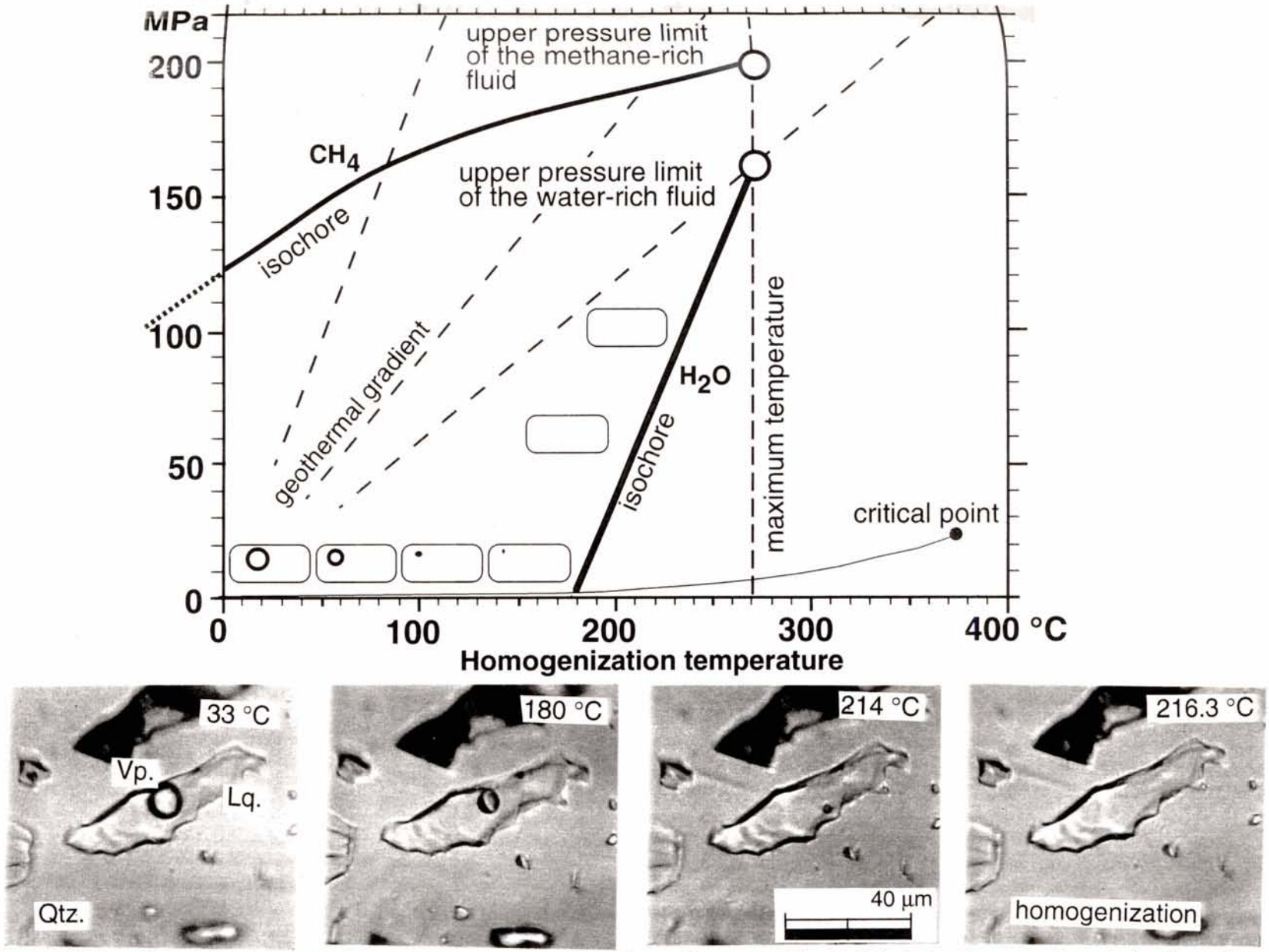

Figure 8. P-T condition determing method. In the heating experiment, the internal pressure of the fluid inclusion increases along the isochore after homogenization. The P-T condition during fluid trapping was somewhere along the isochore. The intersection of the isochore and maximum temperature indicates the maximum pressure of the fluid. The lower limit of the geothermal gradient during fluid trapping can be determined from this intersection and the P-T condition of the sea floor.

fundamental data for calculation of the isochores by Shepherd et al. (1985) for water-rich fluid and Saxena et al. (1987) for methane-rich fluid with computer program by Brown and Hagemann (1989).

3.1 Infrared microspectroscopy

The inclination of the isochore changes by the fluid composition and the concentration of the salt. I obtained them by the infrared spectrum and melting temperature of the fluid.

The infrared spectrum is obtained from clear and large fluid inclusion. The fourier-transform infrared microspectroscopy yields the molecular structural information on individual fluid inclusion larger than 50 μm in size. Some parts of spectral ranges are masked by the strongly absorption of host mineral. The fluid composition is inferred from the remaining spectrum. The systematic diagram and appearance of measuring device are shown in Figure 9. Owing to the infrared beam passes through the air, it is impossible to research the carbon dioxide. The carbon dioxide absorbs strongly, and fluctuation is larger than the other gases within the air.

The infrared spectrums of the two types of fluid inclusions are shown in the Figures 10 and 11. The two phases fluid inclusion in the room temperature absorbs spectrum of the water (Fig. 10). The spectrum of the two phases fluid

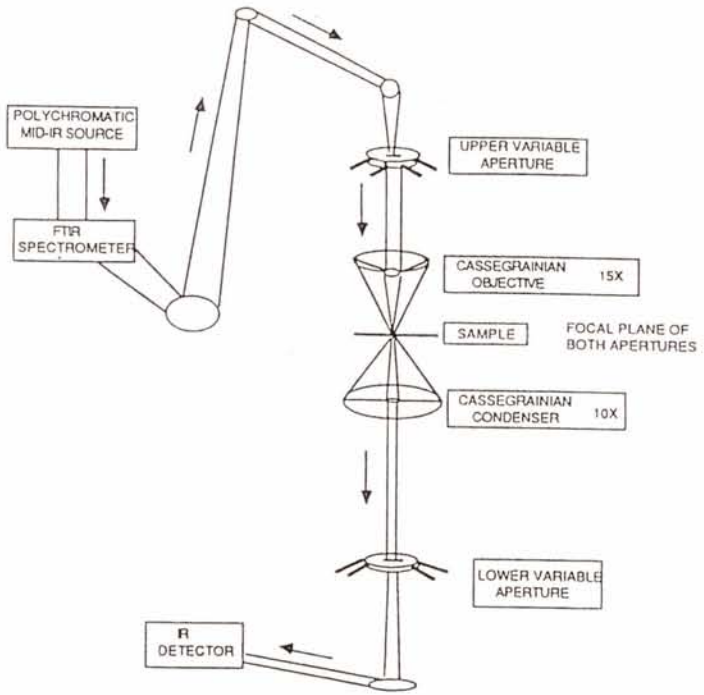

Pironon et al. (1991)

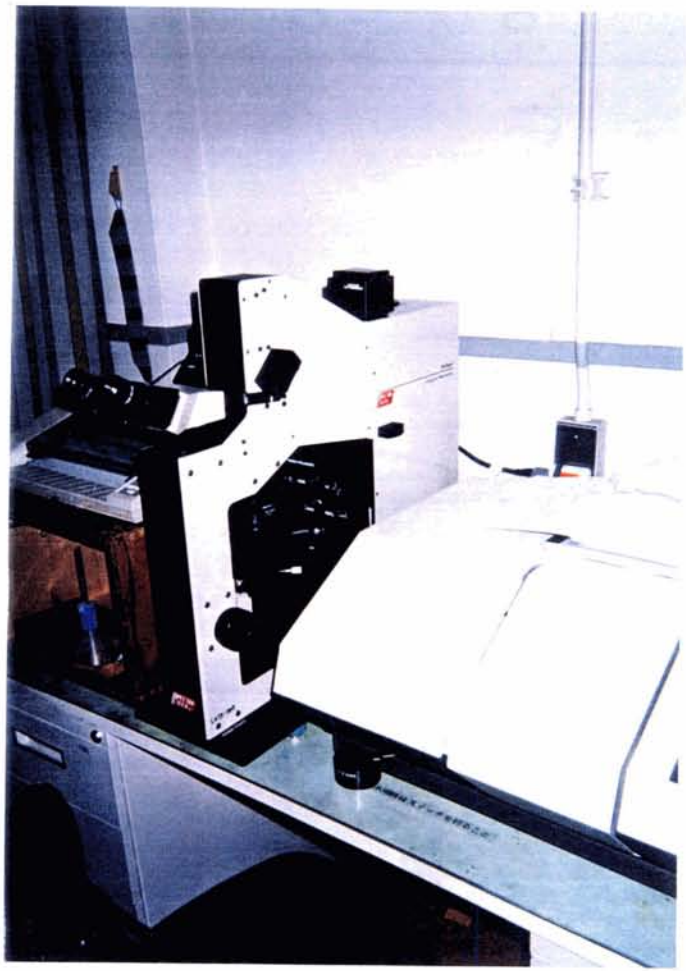

Figure 9. Diagram and appearence of the fourier-transform infrared microspectrometer.

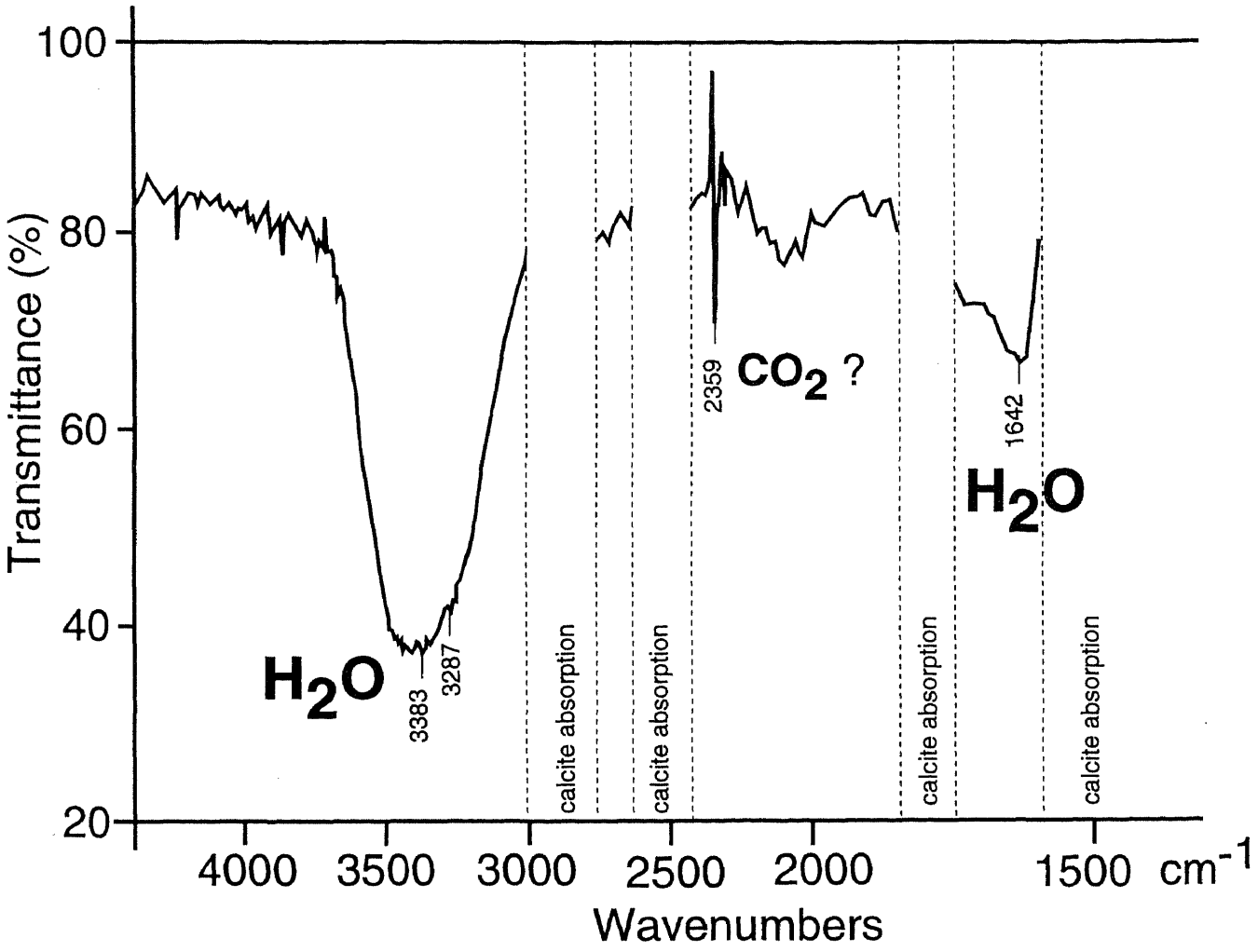

Figure 10. Infrared spectrum of the water-rich fluid inclusion. The infrared was absorbed on the band of the water (H2O) typically.

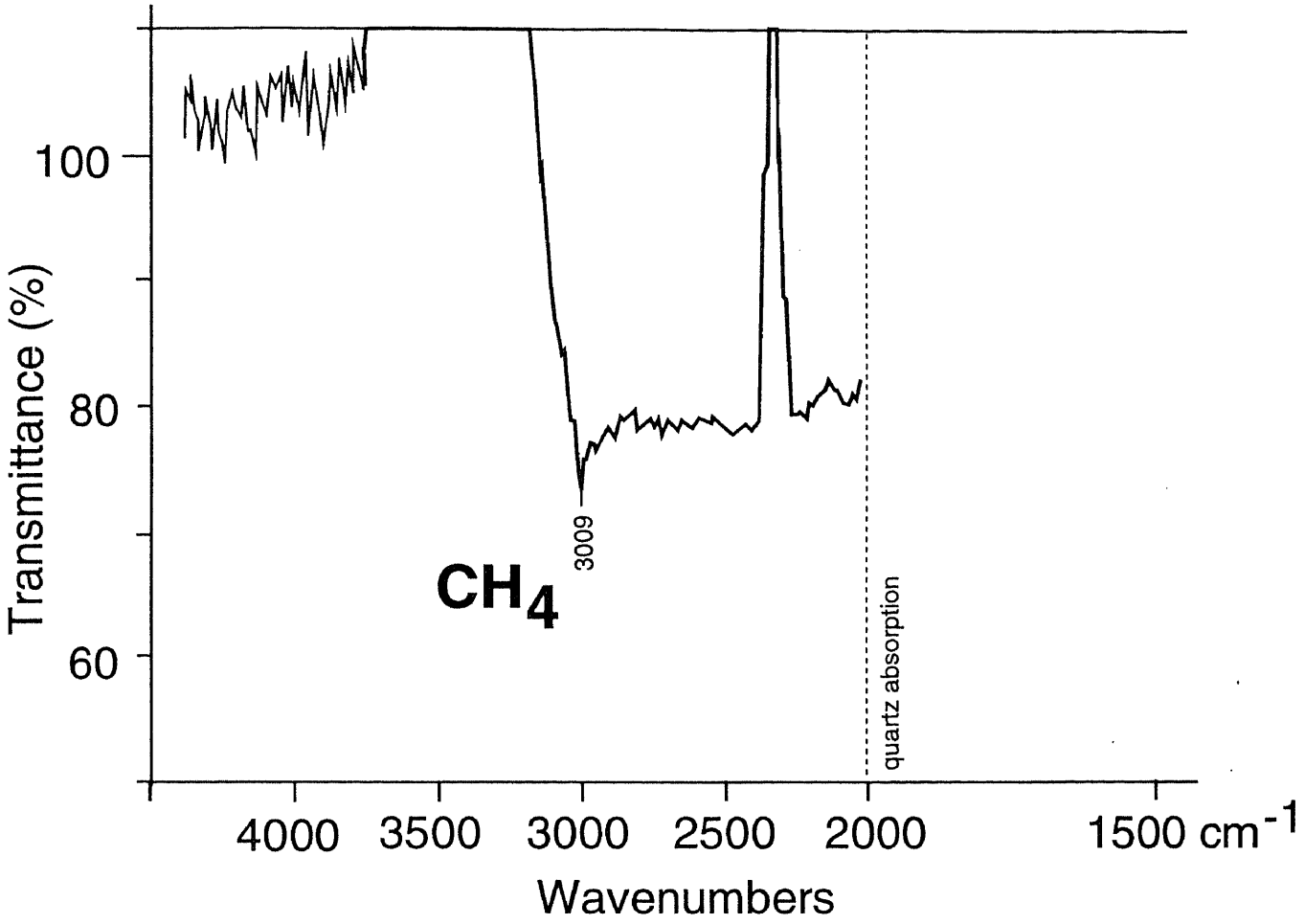

Figure 11. Infrared spectrum of the methane-rich fluid inclusion. It was found that the weak absorption band on the methane (CH4) and negative absorption band on the CO2 and carbon dioxide (CO2). This indicate that this fluid inclusion is rich in CH4 and poor of H2O and CO2. The weak absorption band of CH4 may be owing to the low density.

inclusion in the room temperature is characterized by the absorption band of water typically. In addition, the weakly absorption and the peak transmittance of the infrared are found near the band of carbon dioxide. This indicates that this are influenced suffering by the fluctuation of the carbon dioxide in the laboratory during measuring. The infrared spectrum of the other type fluid inclusion is characterized by the weakly absorption band of methane (Fig. 11) and negative absorption band of water and carbon dioxide. This indicates that the fluid inclusion of this type is rich in methane and poor of the water and carbon dioxide. The weak absorption of the methane band may indicate the low density of the fluid.

The salt concentration of the water-rich fluid inclusion was calculated from the melting temperature by cooling experiment. The dissolved salt lowers the freezing point of the water. The melting temperatures of the water within the inclusions are from -1.4 to -0.2 °C. These correspond with 0.3% to 2.4% of concentration for NaCl (Potter et al., 1978; Sasada, 1989). The fluid has lower salinity than the sea water.

Chapter 4

RESULTS

4.1. Thermal structure of the Chichibu and Shimanto accretionary complexes

As the results of the measurement of the Rmax value, shown in Table 1 data from this area range from 0.9 % to 5.7%. The extraordinary high Rmax values, over 4 % in the southernmost part of this area, might be due to the contact metamorphism.

The southernmost Cretaceous unit in the inland area and the most part of the Tertiary unit in the coastal area have higher Rmax values above 3% (Fig. 2) than the other northern areas. Among them, the highest Rmax value of 5.7% is in the Shimizu Formation near the Ashizuri Granite. I demarcated the boundary of the contact metamorphosed region, approximately 20-50 km in width, by a sharp line as in Figure 2; as the Rmax value suddenly increases to the south from the line. In this region, site of high Rmax is scattered without a characteristic increase trend, and many of thick quartz veins, 5-10 cm in width, ubiquitously occur. Furthermore, this high Rmax region is wider than the area inside of the biotite isograd (Tokunaga, 1992), and the region boundary is discordant with the geologic structures. Although this region might have suffered thermal effect from the igneous activity, it seems that the heat source of this region is not only the Ashizuri Granite, because the high

Table 1. The list of the vitrinite reflectance results.

Sample No.	Rm	Rmax	Rmin	Sample No.	Rm	Rmax	Rmin	Sample No.	Rm	Rmax	Rmin	Sample No.	Rm	Rmax	Rmin
AW1004	1.80	1.87	1.72	OK623	1.75	1.88	1.59	OZ1016	1.33	1.36	1.27	TNN1013	-	1.50	-
AW1006	1.50	1.55	1.45	OK627	1.80	1.89	1.67	OZ1019	2.47	2.61	2.46	TNN1014	-	1.50	-
AW1007	1.54	1.58	1.50	OK633	2.39	2.47	2.31	OZ1021	2.03	2.18	1.90	TNN1015	-	1.90	-
AW1008	1.87	1.94	1.76	OK636	2.31	2.40	2.15	SD1000	1.85	1.91	1.82	TNN1016	-	2.00	-
AW1011	1.89	1.97	1.81	OK644	2.02	2.13	1.88	SD1006	1.24	1.26	1.15	TNN1017	-	1.90	-
AW1012	1.99	2.10	1.92	OK647	1.94	2.01	1.82	SGC0001†	-	0.70	-	TNN1025	2.25	2.39	2.13
AW1013	1.94	1.99	1.86	OK652	1.75	1.85	1.56	SGC0009†	-	0.80	-	TS1000	1.97	2.07	1.89
AW1014	1.86	1.98	1.77	OK660	1.85	2.01	1.70	SGC0010†	-	0.90	-	TS1001	1.73	1.81	1.66
AW1015	2.22	2.34	2.08	OK663a	1.82	1.92	1.72	SK1042*	1.20	-	-	TS1002	1.75	1.83	1.64
AW1016	1.89	2.03	1.75	OK663b	1.79	1.99	1.61	SK1043*	1.26	-	-	TT001*	1.15	-	-
IB1015	-	1.30	1.15	OK672	2.11	2.15	1.96	SK1047*	0.98	-	-	TT002*	1.02	-	-
IB1016	-	1.30	1.19	OK675	2.13	2.24	2.01	SK1048*	1.08	-	-	TT1001*	2.31	-	-
IB1020	-	1.50	1.35	OK678	2.35	2.47	2.18	SK1058*	1.15	-	-	TZC0003†	-	1.40	-
KB1000	2.04	2.10	1.93	OK682	2.33	2.47	2.20	SK1061*	1.12	-	-	TZC0004†	-	1.90	-
KB1001	2.07	2.21	1.95	OK754	2.36	2.50	2.22	SK1063*	1.03	-	-	YH1000	2.37	2.49	2.26
KR1000	2.17	2.26	2.01	OK755	2.25	2.33	2.04	SK1065*	0.95	-	-	YH1001	2.03	2.14	1.91
KR1001	2.29	2.46	2.14	OK801	2.91	3.02	2.79	SK1066*	0.75	-	-	YH1007	1.79	1.91	1.71
KR1002	1.15	1.20	1.10	OK805	3.24	3.45	3.14	SK1072*	1.08	-	-	YH1012	1.71	1.80	1.63
KR1003	1.14	1.17	1.11	OK831	2.86	2.96	2.75	SK1073*	1.09	-	-	YH1015	1.69	1.76	1.62
KR1004	1.40	1.46	1.34	ON1000	4.96	5.60	3.80	SK1074*	1.42	-	-	YH1015	1.69	1.76	1.62
KR1005	1.26	1.31	1.21	OY1004	3.05	3.26	2.83	SK1087*	1.31	-	-	YK1005	2.79	3.14	2.51
OBI0001	-	5.70	-	OY1009	2.95	3.11	2.76	SK1090*	1.48	-	-	YK1007	2.68	-	-
OG1000	1.06	1.08	0.98	OY1017	3.24	3.58	2.79	SK1098*	1.19	-	-	YK1008	2.81	3.07	2.63
OK500	1.94	2.11	1.84	OY1026	2.72	2.88	2.55	SK1099*	0.99	-	-	YK1010	2.63	-	-
OK521	2.97	3.21	2.75	OY1028	3.13	3.26	2.92	SK1101*	1.17	-	-	YK1011	2.53	2.73	2.33
OK531	2.67	2.86	2.59	OY1031	3.21	3.40	3.07	SK1102*	0.99	-	-	YK1016	2.34	-	-
OK534	1.98	2.16	1.78	OY1032	3.27	3.52	2.91	SK1103*	1.06	-	-	YK1032	2.21	-	-
OK541	2.36	2.62	2.18	OY1045	3.13	3.38	2.86	SK1106*	1.07	-	-	YK1033	2.32	-	-
OK542	2.56	2.67	2.38	OY1046	3.20	3.49	2.90	SK1107*	1.21	-	-	YK1035	2.27	-	-
OK543	2.13	2.25	2.00	OY1047	2.88	3.18	2.66	SK1112*	1.12	-	-	YK1037	2.20	-	-
OK545	2.11	2.28	1.92	OY1048	2.93	3.01	2.85	SK1113*	0.99	-	-	YK1038	2.06	-	-
OK547	2.18	2.46	1.99	OY1053	2.35	2.55	2.18	SK1200	1.21	1.27	1.17	YK1038B	2.05	2.13	1.96
OK550	2.67	2.71	2.38	OY1056	2.00	2.11	1.86	SK1201	1.41	1.52	1.36	YK1039	1.96	2.08	1.84
OK552	2.67	2.77	2.59	OY1059	2.47	2.60	2.31	SKC0005†	-	0.80	-	YK1042	1.91	1.91	-
OK565	2.16	2.28	2.04	OY1061	3.14	3.34	2.90	SS001*	1.14	-	-	YK1043	2.71	3.01	2.44
OK566	2.17	2.38	1.99	OY1062	2.27	2.38	2.18	SS603	0.86	0.89	0.82	YK1044	2.71	3.01	2.44
OK567	2.34	2.48	2.18	OY1062f	2.78	3.09	2.56	SS604	1.25	1.36	1.18	YK1054	3.06	3.30	2.81
OK569	2.56	2.67	2.40	OY1064	2.71	3.06	2.47	SS610	1.53	1.60	1.45	YK1055	2.89	3.32	2.60
OK570	2.45	2.60	2.30	OY1065	2.87	3.12	2.66	SS612	1.24	1.28	1.20	YK1056	2.77	3.09	2.55
OK573	2.25	2.44	2.09	OY1066	2.87	3.06	2.65	SS613	1.41	1.44	1.35	YK1061	2.61	2.80	2.42
OK575	2.17	2.38	2.00	OY1067	2.81	3.00	2.61	TN1000	1.19	1.22	1.14	YK1066	2.60	2.89	2.42
OK577	2.24	2.44	2.08	OY1074	2.51	2.67	2.36	TN1001	1.27	1.32	1.23	YK1069	2.67	2.88	2.52
OK579	2.62	2.85	2.38	OY1075	2.46	2.77	2.28	TN1002	4.62	5.35	3.98	YK1088	2.53	2.80	2.34
OK580	2.74	2.94	2.51	OY1078	2.01	2.09	1.91	TN1004	2.98	3.20	2.78	YK1089	2.76	3.05	2.37
OK583	2.48	2.78	2.27	OY1079	2.25	2.35	2.14	TN1018	3.77	4.12	3.41	YK1093	3.00	3.33	2.72
OK588	2.16	2.30	2.02	OY1081	2.34	2.54	2.21	TN1021	3.18	3.42	2.80	YK1094	2.93	3.13	2.64
OK597	1.87	1.97	1.77	OY1083	1.95	2.09	1.81	TN1022	3.96	4.67	3.34	YK1096	2.73	3.00	2.53
OK602	2.07	2.17	1.97	OY1084	2.12	2.18	2.04	TN1025	3.73	4.50	3.26	YK1099	3.02	3.10	2.65
OK605	1.98	2.11	1.89	OY1085	1.70	1.77	1.61	TNN1003a	1.25	1.30	1.24	YK1108	2.99	3.27	2.70
OK607	1.78	1.84	1.67	OZ1001	1.11	1.17	1.06	TNN1004	1.51	1.56	1.45	YK1115	2.75	3.03	2.42
OK610	1.92	2.00	1.81	OZ1005	1.06	1.14	1.00	TNN1006	1.59	1.67	1.51	YK1117	2.60	2.97	2.30
OK614	2.01	2.18	1.83	OZ1006	3.03	3.36	2.74	TNN1007	1.52	1.56	1.46	YK1118	2.73	2.82	2.41
OK617	1.49	1.56	1.40	OZ1008	3.27	3.56	2.97	TNN1009	1.48	1.51	1.43	YK1120	2.80	3.11	2.37
OK619	1.41	1.48	1.33	OZ1010	1.86	1.93	1.77	TNN1011	-	1.90	-	YK1121	2.32	2.45	2.21
OK621	1.63	1.73	1.51	OZ1011	1.86	1.96	1.77	TNN1012	-	1.60	-				

*Ohmori (1994)
†Okano (1992)

temperature around the Ashizuri Granite is not concentric. The early Miocene Misaki Group (Kimura, 1985), older than the Ashizuri Granite, avoids extraordinary high temperature in spite of the group overlying the high Rmax region. It is likely that the latent igneous body or localized hydrothermal activity might make such an un-concentric high Rmax region. I dispensed this region from the following discussion.

The sampling points, Rmax values and general trend of the non-contact metamorphosed area are shown in Figures 1 and 12. At the beginning, I will examine the detailed thermal structure of some selected area such as around the Yokonami Melange and BTL.

The Rmax values of the Yokonami Melange and surrounding strata in the Goshikigahama area are shown in Figure 13. The boundary between the Yokonami Melange and Susaki Formation is not only the lithologic boundary but also the chronological boundary. There are several decades of million years of age difference between the Shinjogawa Group and Taisho Group (Okamura, 1991). However, the Rmax in Yokonami Melange does not differ with the surrounding strata. In addition, both sandstone blocks and black shale matrix within the melange units have equal Rmax values each other (Fig. 13). The same observation is applied in the Awa area, western extension of the Goshikigahama area, although the Rmax values are lower than the Goshikigahama area. Similarly, the Kure Melange has equal Rmax with the Shimotsui Formation (Fig. 12). As a result, generally the Rmax value in the

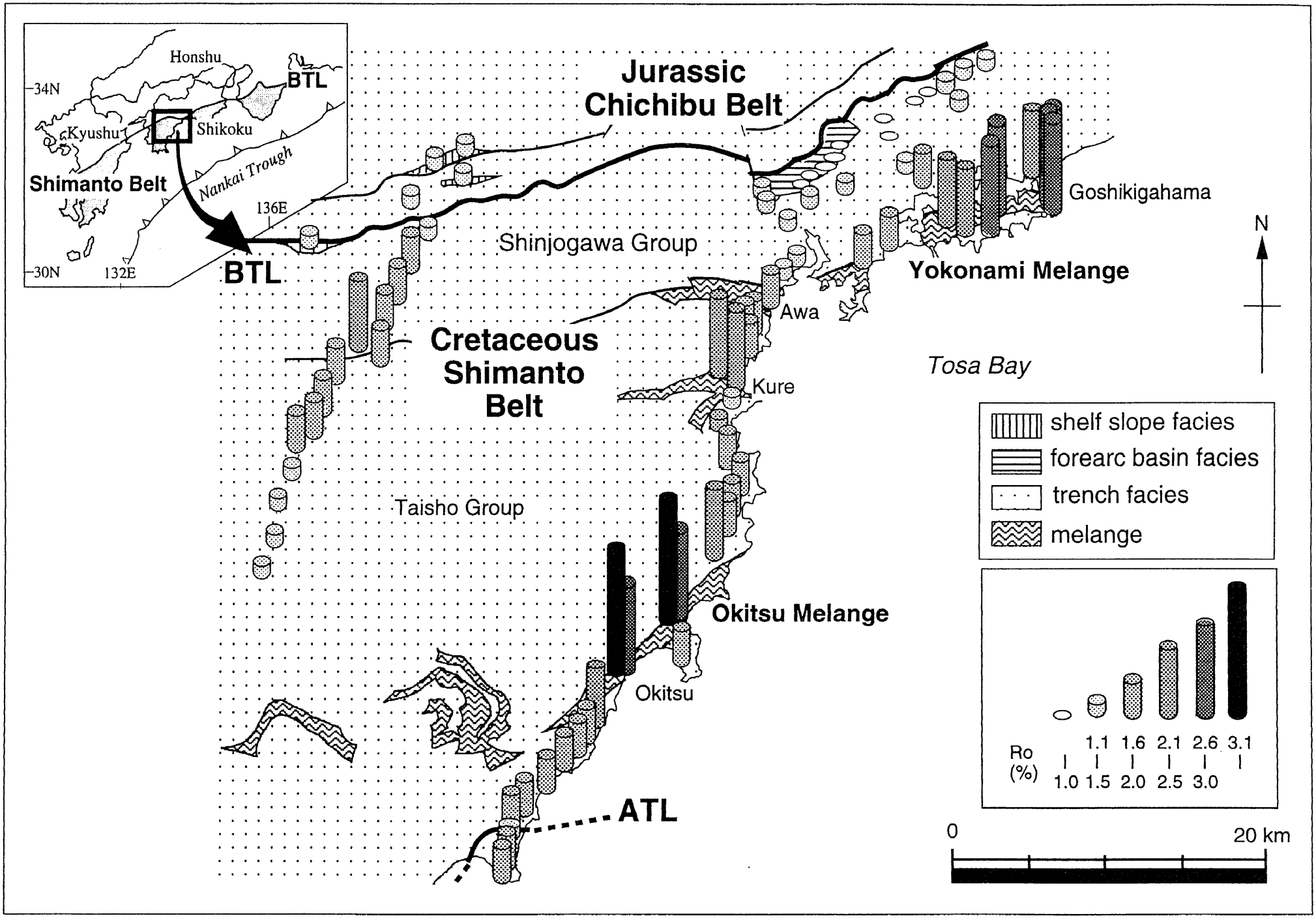

Figure 12. General trend of the vitrinite reflectance in the Cretaceous unit. The longer and red column indicates higher Rmax.

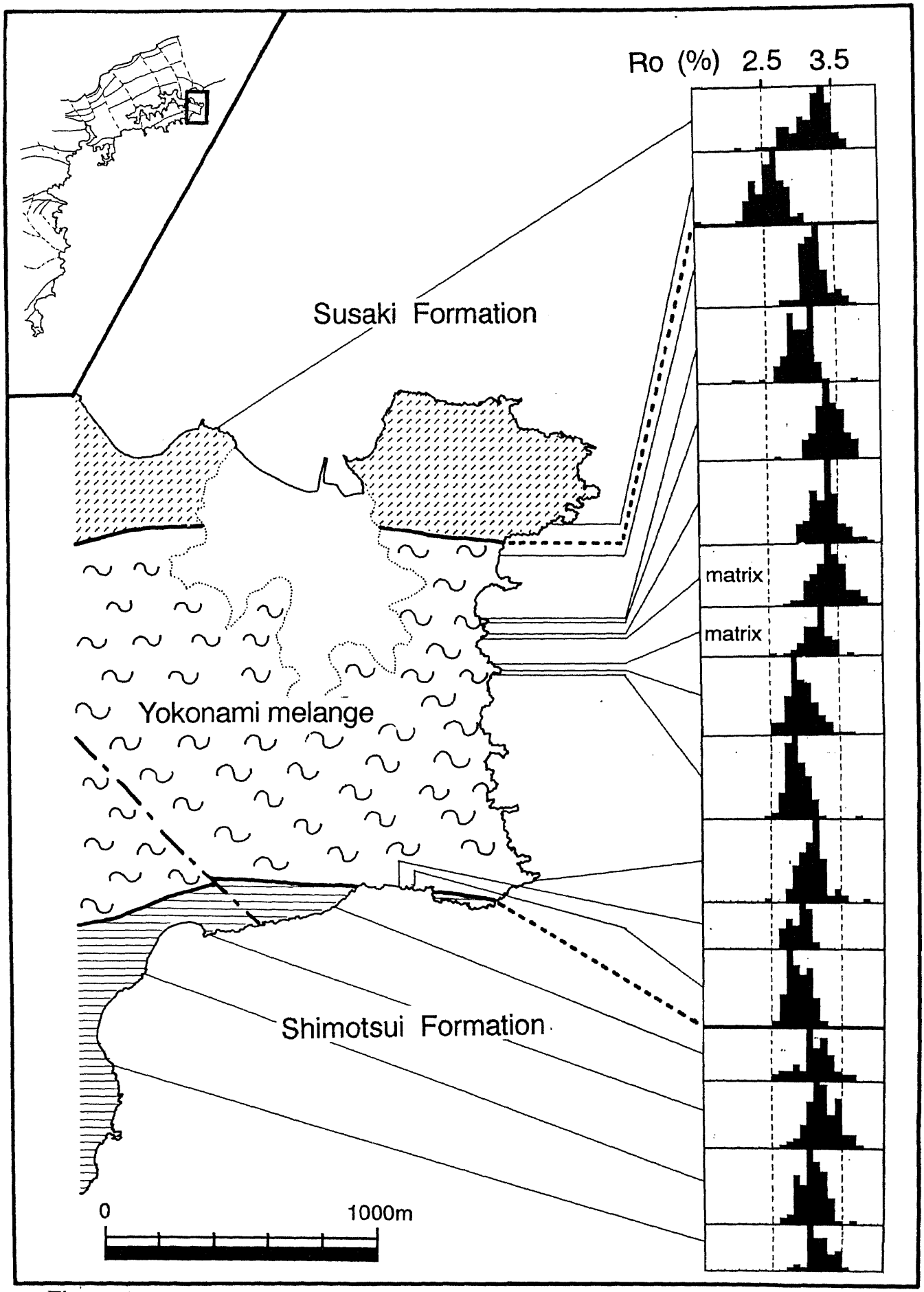

Figure 13. Detailed thermal structure around the Yokonami Melnage. The maximum vitrinite reflectance (Rmax) value between the melange and the surrounding trench facies is continuous. In addition, both sandstone blocks and black shale matrix within melange has equal Rmax value each other.

melange and surrounding strata are of the same level except for the Okitsu Melange.

The Rmax value of the Jurassic to Cretaceous rocks in the inland area near the BTL is shown in Figure 14. The trend of Rmax is continuous, although this area is composed of sediments of various facies such as the Jurassic trench facies, Cretaceous trench facies, Cretaceous forearc facies and Cretaceous shelf facies. The Rmax increases from 1.2% to 1.8%, penetrating throughout all the various facies, ages and BTL. Thus, the important point is that the thermal structure is independent of the geologic structure, and even the shelf facies suffered high temperature. The Rmax values of 1.2-1.4 % in the Monobegawa and Torinosu Groups are as high as in the surrounding Jurassic formation of the Chichibu accretionary complex.

Next, I will consider the thermal structure from a wider point of view. In the coastal area, the trend of the Rmax value is characterized by the repeated southward increase with a remarkable spike at the Okitsu Melange. Schematic cross section with Rmax is shown at bottom of Figure 15. The value of Rmax increases continuously from the BTL to the Kure Melange, from 1.0% to 2.2%. This southward increase trend is regardless of the geologic structure. The value of the Rmax drops rapidly to 1.1% at the south of the Kure Melange, and increases southward again to 2.2%. This thermal boundary disagrees with the chronological and major tectonic boundaries (Fig. 15). The Kure Melange and Nonokawa Formation that are on both sides of this thermal

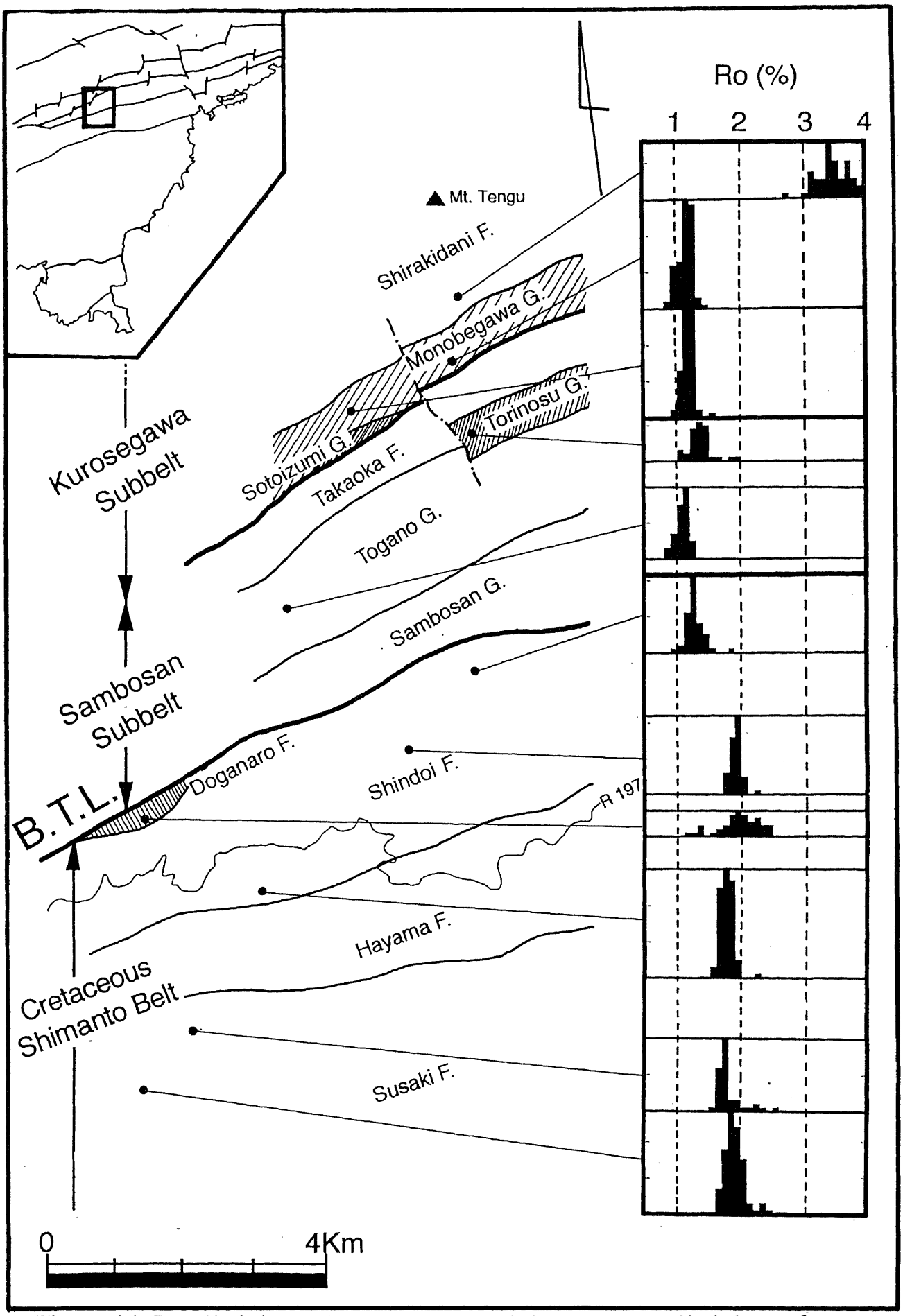

Figure 14. Detailed thermal structure around the BTL. Detailed thermal structure around the BTL. The thermal structure is continuously, eventhough there are various sediments such as middle Cretaceous forearc sediment and upper Cretaceous shelf sediment on the Jurassic to lower Cretaceous trench fill sediment. This indicates that the thermal structure was formed after the accretion.

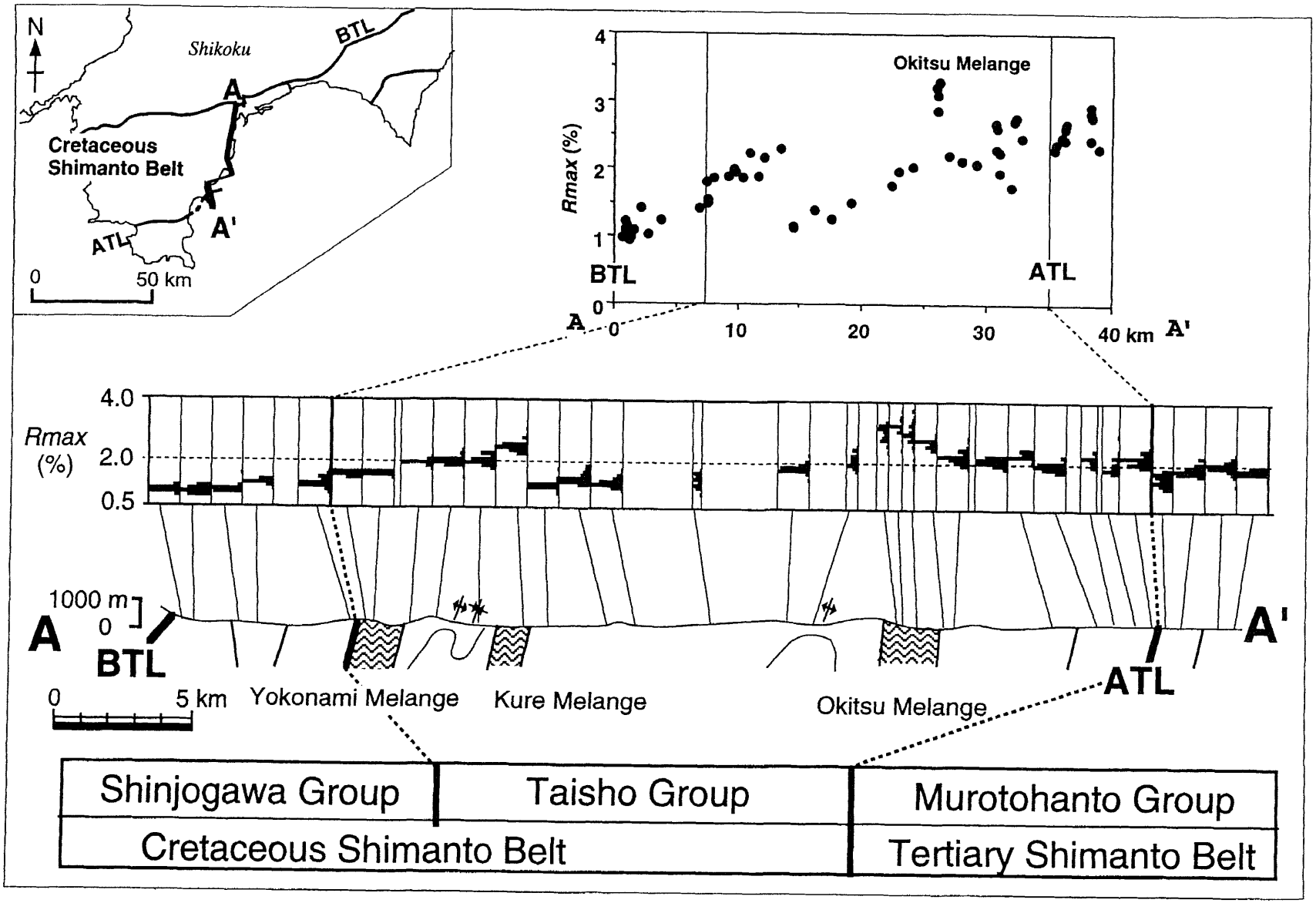

Figure 15. Thermal structure and geologic cross section. Geologic cross section with Rmax. Cretaceous Shimanto Belt has a thermal structure of simple southward increase, dislocated by late faults, with exceptional peak only at Okitsu Melange.

boundary are contemporary (Taira et al., 1980).

Thus, seaward increase trend of the Rmax may be ubiquitous throughout the Chichibu to Shimanto accretionary complexes whole in southwest Japan. The similar trend was also reported in the eastern Shikoku and Kyushu areas (Mori and Taguchi, 1988; Murata, 1996; Kumon, 1992; Ohmori et al., 1994). However, the south of inland area in western Shikoku has southward decrease trend exceptionally. The Rmax in the inland area increases southward from 1.1 % in the Jurassic Chichibu complex to 2.5 % in upper Cretaceous complex and then decreases to 1.2% (Figs. 1 and 2).

Only the Okitsu Melange does not integrate into the continuous thermal structure. The Okitsu Melange has much higher Rmax than the surrounding strata (Fig. 16). The Rmax value increases rapidly to 3.1 % on the boundary with the Okitsu Melange of 1 km in width (Fig. 16). In the south of the Okitsu Melange, the Rmax is maintained a high value of 2.0 % except a slight decrease on the ATL (Fig. 15).

It becomes clear that the Jurassic to Cretaceous units have a simple shape of the thermal structure regardless of the early-phase geologic structure. The Rmax also changes along the strike of the formations. For example, the Rmax value of the Yokonami Melange and surrounding strata increases eastwards from 1.6 to 2.8 % (Fig. 12)(Sakaguchi, 1996).

The schematic thermal structure of the belts except contact metamorphosed region is shown in Figure 17. The thermal structure of this area can be

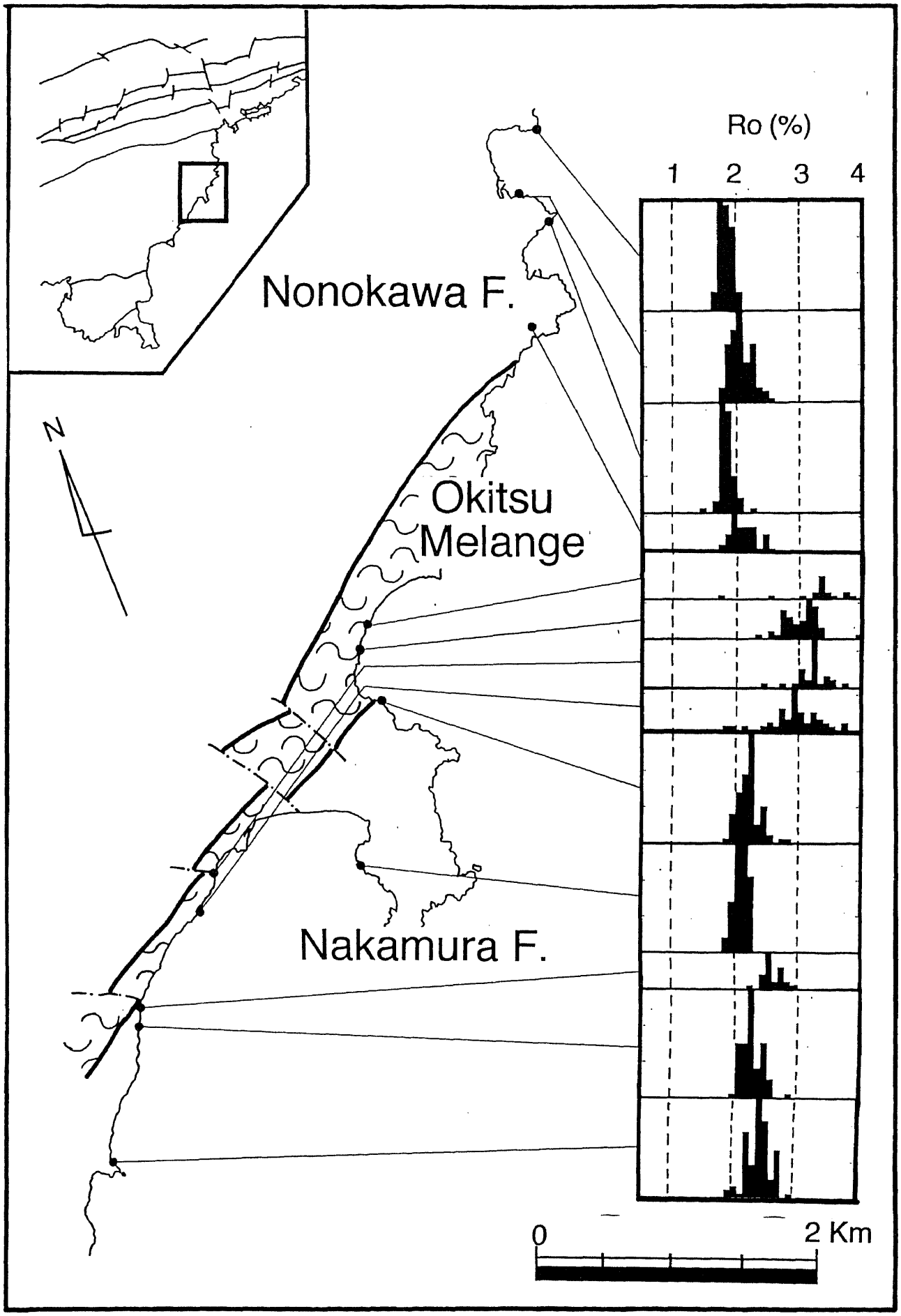

Figure 16. Detailed thermal structure around the Okitsu Melnage. The Rmax value increases rapidly to 3.1 % on the boundary with the Okitsu Melange of 1 km in width.

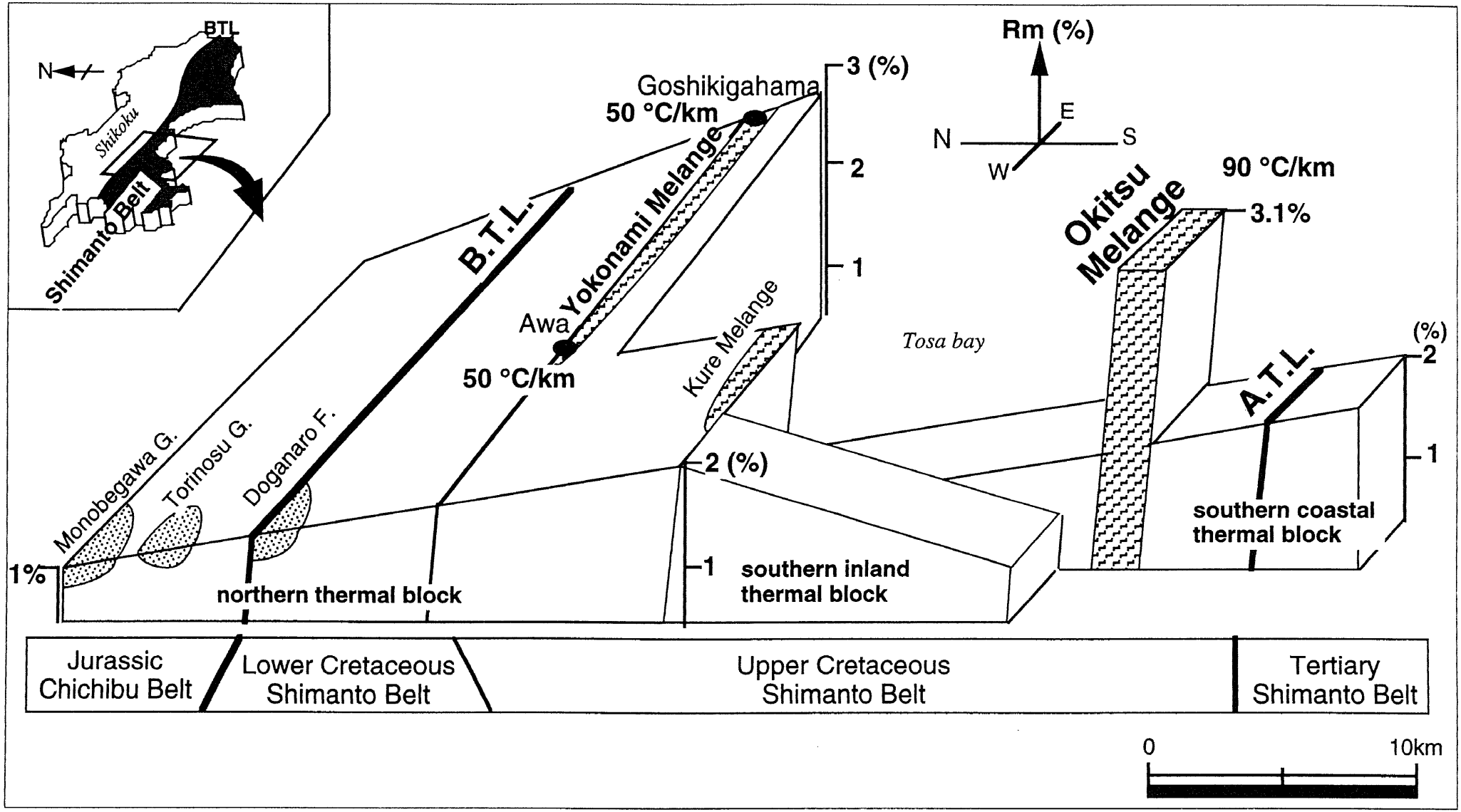

Figure 17. The schematic thermal structural model. This model expresses higher Rmax by height. The thermal structure of this area can be classified into four thermal blocks. The height of this model indicates uplift quantity except the Okitsu Melange and surrounding strata. Because, these were undergone higher geothermal gradient than northern area.

classified into four thermal blocks by thermal continuity; the northern part, southern coastal part, southern inland part and the Okitsu Melange (Fig. 17). These thermal blocks except the Okitsu Melange are similar each other in the shape and size, 10 to 15 km in length. However, only the southern inland block has northward increase trend. The important point to notice is that the height of this model illustrates the relative quantity of the uplift except the Okitsu Melange, because the Okitsu Melange has an extraordinarily high geothermal gradient (Sakaguchi, 1996).

4.2. Homogenization temperature of the water-rich fluid inclusions

Veins of the Yokonami Melange were collected from both the Awa and Goshikigahama areas. Each vein is composed of calcite and quartz small veins, however, the homogenization temperature values are consistent throughout all the directions and all the minerals in the same area. All the histograms of the homogenization temperature values are well concentrated, and the values differ from location to location. In general, the area with higher Rm values has higher peak value of homogenization temperature (Fig. 18). This coincidence indicates that the most of fluid inclusions were trapped during the peak of the thermal history. Moreover, the southern area has higher homogenization temperature than the northern area with the same Rm,

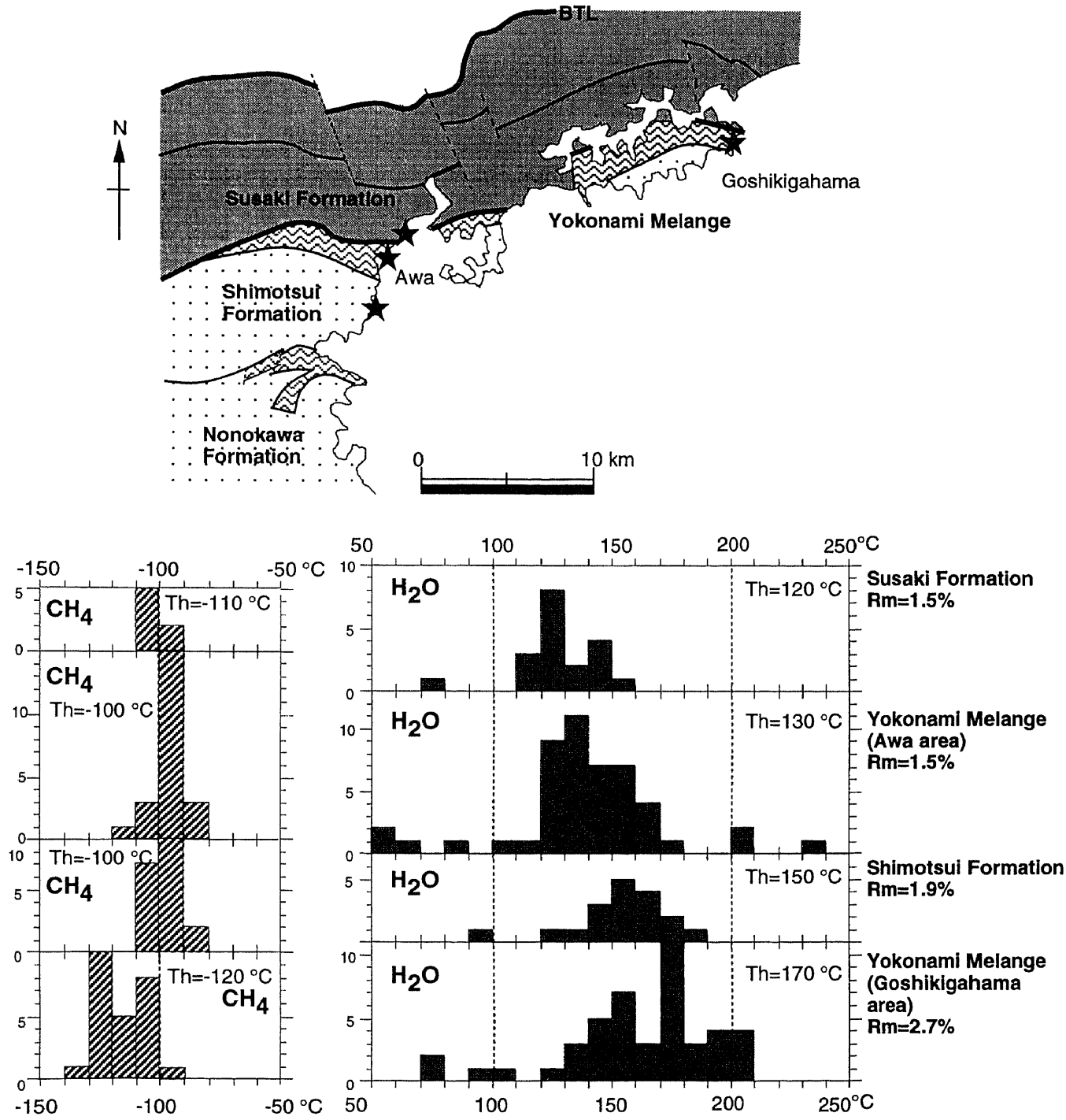

Figure 18. Sampling point and homogenization temperature of the water-rich and methane-rich fluid inclusions. A quartz and calcite vein sampling site and the homogenization temperature (Th) of the water-rich and methane-rich fluid inclusions. In generally, the area with higher mean vitrinite reflectance (Rm) has higher Th of water-rich fluid inclusion.

suggesting that the southern area suffered high temperature with low pressure.

The peak values of the homogenization temperature histograms are 120 °C in the Susaki Formation, 140 °C in the Awa area, 180 °C in the Goshikigahama area of the Yokonami Melange, 150 °C in the Shimotsui Formation, 170 °C in the northern Nonokawa Formation, 210 °C in the southern Nonokawa Formation and 210-220 °C in the Okitsu Melange (Fig. 18).

4.3. Homogenization temperature of the methane-rich fluid inclusions

The homogenization temperature of the methane-rich fluid inclusions were measured in the Yokonami Melange and surrounding strata of the Susaki and Shimotsui Formation. The fluid inclusions from the Yokonami Melange were measured in the Awa area and Goshikigahama area. In general, the quartz that involves methane-rich fluid inclusion, does not have primary water-rich fluid inclusion, but the secondary (Fig. 7b). The homogenization temperatures of the methane-rich fluid inclusion values are consistent throughout all the directions and all the minerals in the same area as same as water-rich fluid inclusions. All the histograms of homogenization temperature values indicate the same peak of -100 °C with quite concentration except Goshikigahama area of -120°C. The relationship between the homogenization temperature and

vitrinite reflectance is found in the water-rich fluid inclusions, but not in the methane-rich fluid inclusions.

All the methane-rich fluid inclusions have the same homogenous temperature within the same sample, but one quartz grain involves the inclusions that have various homogeneous temperatures. The homogenous temperature of them increase rimward of the crystal from -111 °C to -99 °C (Fig. 19). This quartz grain is less than 0.5 mm in size and these fluid inclusions are scattered inside of 0.1 mm square. This changing trend of the homogenization temperature within the one mineral grain indicates that this crystal grew during the P-T evolution of the fluid.

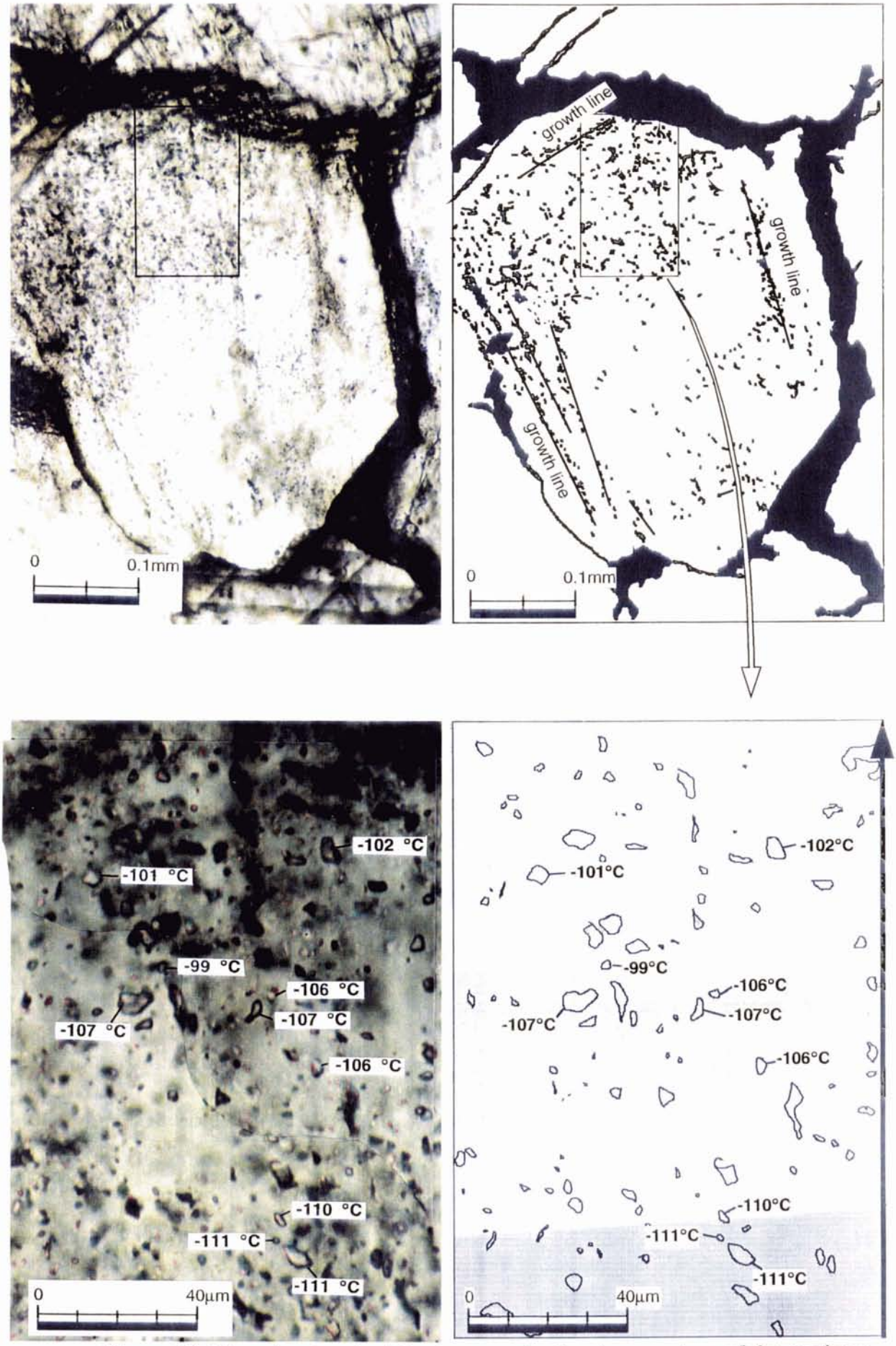

Figure 19. Changing trend of the homogenization temperature of the methane-rich fluid inclusion with crystal growth.

Chapter 5

DISCUSSIONS

5.1. Estimation of the P-T conditions and paleo-geothermal gradient

First of all, I will determine the P-T conditions of the fluids, which as fundamental data for the following discussions. As mentioned in the previous chapter, the P-T condition during fluids trapping is obtained from the method of intersection of the isochore and maximum temperature, and the results are shown in Table 2 and Figure 20. As an opposition to water-rich fluid, for the methane-rich fluid not only the maximum limit but also minimum limit of the trapping P-T condition, because the isochore of the methane crosses the axis of the 0 °C that is the lowest temperature for the sediment below sea floor.

The obtained maximum P-T conditions of the water-rich fluid is different between the northern thermal block and southern inland thermal block. The value is from 190 (±30) °C/ 95 (±50) MPa to 250 (±30) °C/ 125 (±40) MPa in the former area and from 175 (±30) °C/ 10 (±50) MPa to 265 (±30) °C/ 80 (±40) MPa in the latter area. Among the southern coastal thermal block, the value of fluid trapping pressure in the Nonokawa Formation is lower than the error. This indicates that the southern coastal thermal block suffered higher geothermal gradient or the mode of heating was differ from the northern thermal block.

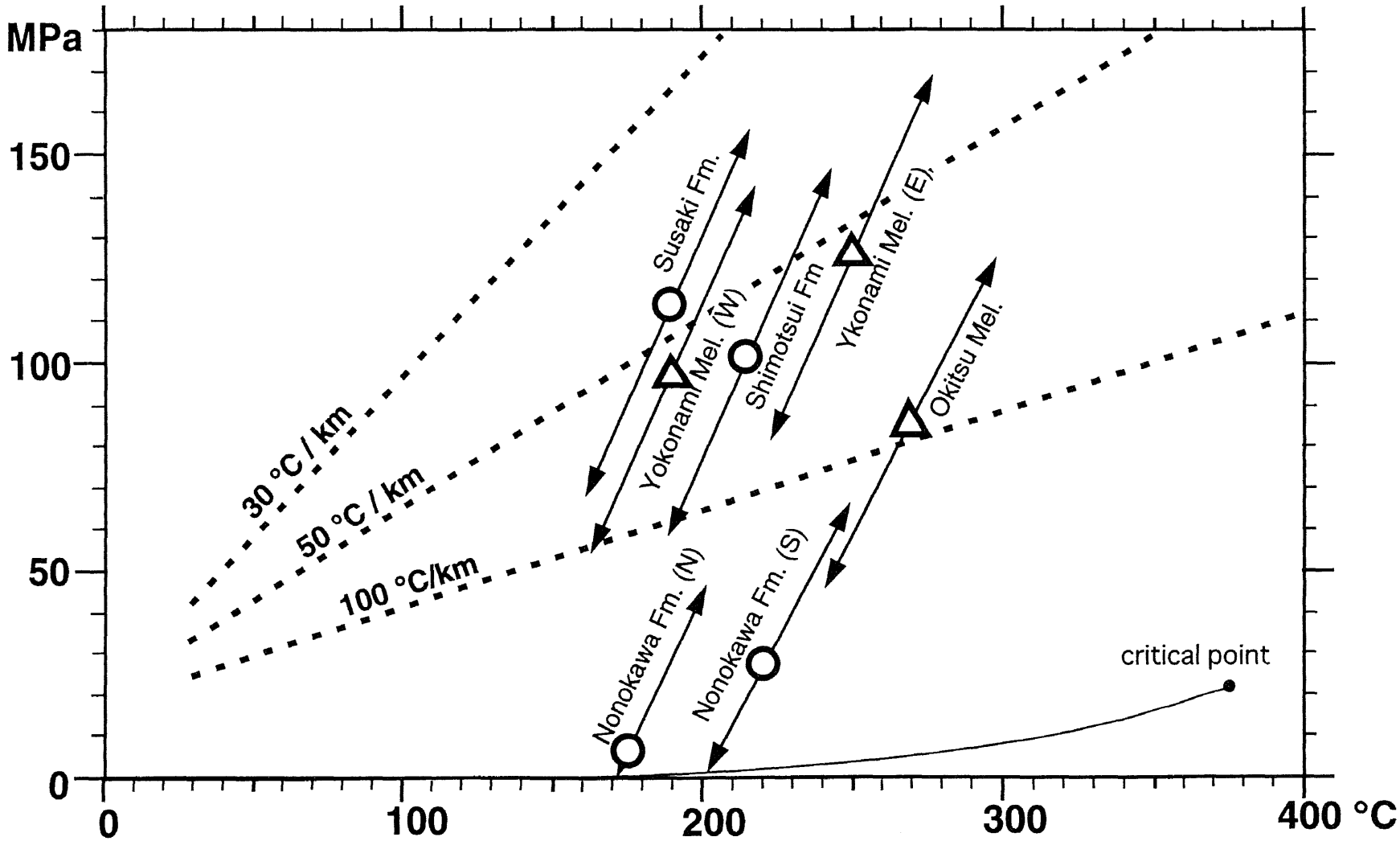

Figure 20. P-T condition during the water-rich fluid trpping. The paleo-geothermal gradient during fluid trapping. The geothermal gradient of all formations and melanges are at least twice times higher than the normal geothermal gradient of 50 °C/km. Among them, the southern part rocks of Nonokawa Formation and Okitsu Melange was undergone the extraordinary high geothermal gradient over 90 °C/km.

Table 2. The homogenization temperature of the water-rich fluid inclusion and the estimated P-T condition and geothermal gradient during fluid trapping.

	Th (water)	Rm	temp. (max)	pressure (max)	depth	geothermal gradient
Susaki Fm.	120 °C	1.5%	190 (±30) °C	110 (±50) MPa	4.2 (±2.2) km	45 (+31/-11) °C/km
Yokonami Mel. (Awa)	130 °C	1.5%	190 (±30) °C	95 (±50) MPa	3.5 (±2.2) km	54 (+60/-16) °C/km
Yokonami Mel. (Goshiki.)	170 °C	2.7%	250 (±30) °C	125 (±50) MPa	4.8 (±2.2) km	52 (+29/-12) °C/km
Shimotsui Fm.	150 °C	1.9%	215 (±30) °C	100 (±50) MPa	4.1 (±2.2) km	52 (+40/-14) °C/km
Nonokawa Fm. (N)	170 °C	1.3%	175 (±30) °C	10 (±50) MPa	-	-
Nonokawa Fm. (S)	200 °C	2.0%	220 (±30) °C	30 (±40) MPa	-	-
Okitsu Mel.	210 °C	3.1%	265 (±30) °C	80 (±40) MPa	2.9 (±1.8) km	91 (+104/-29) °C/km

On the other hand, the P-T condition of the methane-rich fluid was from 0 °C/ 75 MPa to 250 (±30) °C/ 260 (+20) MPa, although the data were obtained from only the northern thermal block (Fig. 21 and Table 3). The trapping pressure of the methane-rich fluid is higher than the water-rich fluid, and there is no P-T difference between the Yokonami Melange and the surrounding strata in either fluids.

The geothermal gradient is estimated from the P-T difference between the sea floor and deeper portion below sea floor. Let us consider the problem of the P-T condition in the sea floor and burial depth of the rock.

The line that joins each point of the upper P-T limit of the water-rich fluid of the northern thermal block in Figures 20 and 21, does not pass through the origin of the coordinates. This line cuts the 0° C axis at ~20 MPa. This result can be explained by the pressure exerting a 2000 m column of sea water over the sediment.

I presumed the bulk density and the pore-fluid pressure as follows. The bulk density of the Nankai accretionary prism from sea floor to 1300 m below sea floor (mbsf) is 1.5 to 2.5 g/cm^3 (Taira et al., 1991). The bulk density under the 1300 mbsf below the sea floor is presumed 2.5 g/cm^3, because that of the Shimanto Belt at present is 2.6 g/cm^3 (Hada, 1988). The pore-fluid pressure increases with depth (Shi and Wang, 1985) and rises to 90% of lithostatic pressure as exemplified at the decollement zone in the present Barbados accretionary prism at 600 mbsf with effective pressure only 8 MPa

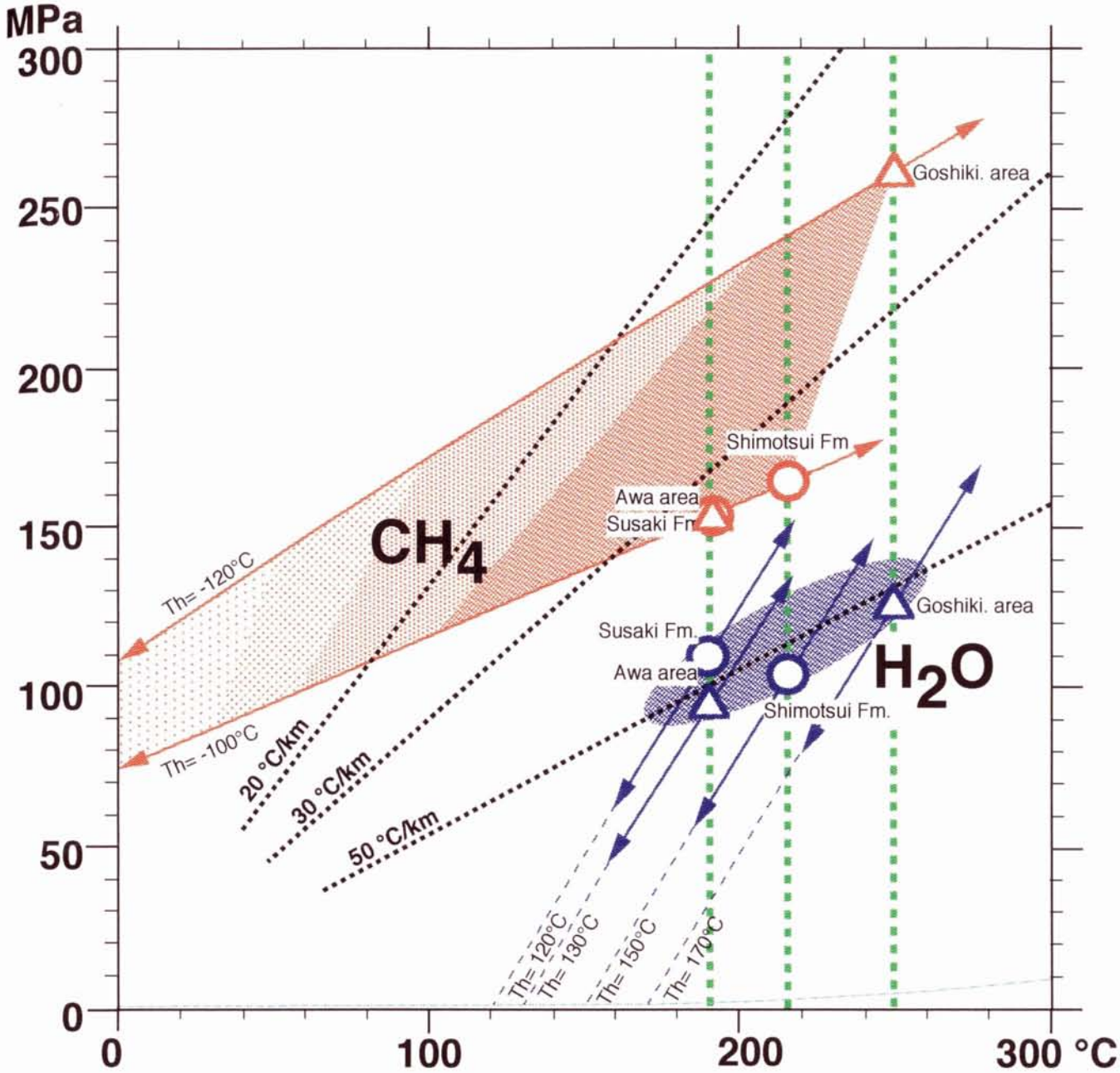

Figure 21. P-T condition during the methane-rich fluid trapping. The methane was trapped at higher pressure of 75-260 MPa with low geothermal gradient of ~33°C/km than the water trapping condition.

Table 2. The homogenization temperature of the methane-rich fluid inclusion and the estimated P-T condition and geothermal gradient during fluid trapping.

	Th (methane)	Rm	temp. (max)	pressure	depth	geothermal gradient
Susaki Fm.	-110°C	1.5%	190 (±30) °C	90-155 MPa	3.3-6.1 km	< 31 °C/km
Yokonami Mel.	-100°C	1.5%	190 (±30) °C	75-155 MPa	2.6-6.1 km	< 31 °C/km
Yokonami Mel.	-120°C	2.7%	250 (±30) °C	110-260 MPa	4.2-10.6 km	< 24 °C/km
Shimotsui Fm.	-100°C	1.9%	215 (±30) °C	75-165 MPa	2.6-6.5 km	< 33 °C/km

(Moore et al., 1995). Even though the decollement zone is unique, the pore fluid pressure in the deeper portion, over 80 MPa as this area, may close to lithostatic pressure. I presumed that the pore-fluid pressure was 90% of lithostatic pressure.

The lower limits of the paleo-geothermal gradients during water-rich fluid trapping are estimated as 45 (+31/ -11) °C/ km to 54 (+60/ -12)°C/ km in the northern thermal block, and over 90 (+91/ -29) °C/km in the southern coastal thermal block (Fig. 21 and Table 2). The geothermal gradient in the southern coastal thermal block is higher than the northern thermal block. Among them, the geothermal gradient in the Nonokawa Formation is too high to estimate by this method, because the obtained fluid pressure is lower than the error.

I infer that the water-rich fluid was trapped during peak heating, because the increase trend of the homogenization temperature has correlation with the Rm. Moreover, the maximum P-T condition of the fluid of the all formations in the northern thermal block are plotted on the same line of approximately 50 °C/ km. Namely, rocks in the northern thermal block reached the maximum temperature under low pressure environment at the same time and the circulation of the water-rich fluid occurred within the accretionary prism at that time.

Thus the values of geothermal gradients are at least twice times higher than the normal geothermal gradient. Let us examine the validity of this result

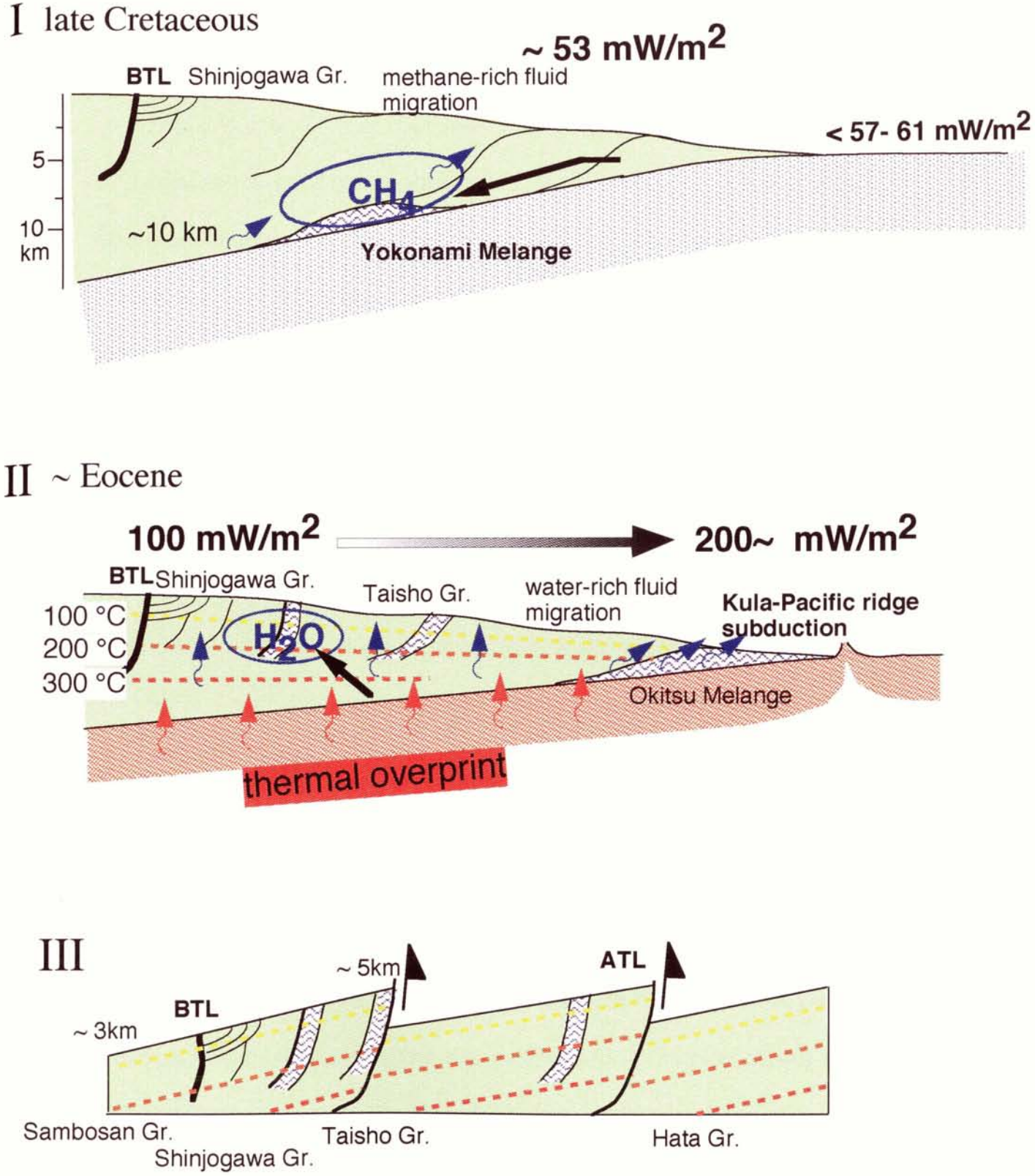

Figure 22. Thermal evolution in the Cretaceous Shimanto accretionary prism.

from differential point of view.

Hibbard et al. (1993), Chijiwa et al. (1988) and Suzuki et al. (1982) estimated paleo-geothermal gradient of the slope basin sediments in the Shimanto accretionary complex based on the maximum temperature and thickness of the slope basin sediment. Though this method can be used only the slope basin with the supposition of the burial depth, it must be checked on the validity of estimation. The geothermal gradient of the Monobegawa and Torinosu Groups as 40 to 45 °C/km is estimated by this way, based on the random Rm of 1.1 to 1.3% as it, corresponds to 160-180 °C and 4 km of assumed burial depth which is the thickest for slope basin (Hibbard et al., 1993). This geothermal gradient is close to the above result.

Next, I will discuss the thermal environment during methane-rich fluid trapping. It is hard to determined the geothermal gradient during methane-rich fluid trapping closely as opposed to the water-rich fluid in the northern thermal block, because the methane might be trapped at differential stage of peak heating. The obtained broad result that from 0 °C/ km to 33 °C/ km can be confined by other information. The obtained upper limit of geothermal gradient in the Goshikigahama area of 24 °C/ km is lower than the Awa area of 31 °C/ km in spite of the same unit. It is likely that there is no difference in geothermal gradient within the same unit during the same stage. The result in the Goshikigahama area may be nearer to the true paleo-geothermal gradient and P-T condition during the methane-rich fluid trapping in Yokonami

Melange than the result in the Awa area. Additionally to this, the geothermal gradient lower than 5 °C/ km is unknown in the earth. Therefore, the paleo-geothermal gradient at the stage of methane-rich fluid trapping is from 5 °C/ km to 24 °C/ km with error of 3 °C/ km.

5.2. P-T path in the Shimanto accretionary complex

It was observed in previous discussion that the water-rich fluid was trapped at peak heating stage with high geothermal gradient under the lower pressure than the methane-rich fluid trapping condition. This illustrates that the each fluid records the differential stage of metamorphism. I would like to discuss the P-T path in the northern thermal block from the P-T condition of each fluid.

Judging from the following evidence, as we have seen, the methane-rich fluid was trapped at earlier stage than water-rich fluid. Firstly, the thermal structure is independent of the geologic structure. This demonstrates that the thermal structure was formed by overprint after the accretion. To sum up, the Shimanto accretionary complex reached the peak temperature at far later stage. Secondary, the increase trend of the homogenization temperature of the water-rich fluid inclusion is correlated with the increase trend of Rm. This indicates that the water-rich fluid was trapped during the peak heating.

Thirdly, the methane-rich fluid was trapped under the higher pressure than the water-rich fluid. Finally, the methane-rich fluid inclusion occurs within the quartz grain that has comb structure, and the calcite vein with water-rich fluid inclusion is deposited between the quartz grain. Thus resulted the P-T path is shown in Figure 22. The rock reached to the highest pressure of 110-260 MPa under geothermal gradient lower than 24 °C/ km, and then underwent peak heating with increase of geothermal gradient to 50 °C/ km at 95-125 MPa.

Next, I will discuss the peak heating time. It was revealed that a young plate subducted beneath the Shimanto accretionary prism at least twice as the latest Cretaceous to Eocene Kula-Pacific plate and middle Miocene Shikoku basin based on the paleo-magnetic data of the oceanic plate and radiolarian age data on the top of it (Seno and Maruyama, 1984; Seno, 1988; Hibbard and Karig, 1990, Engebretson et al., 1985; Maruyama and Seno, 1986; Byrne and DiTullio, 1992, Taira et al., 1988). Overall, the middle Miocene event was much more pronounced, with granitic plutonism and volcanism occurring throughout southwest Japan; however, the pre-Miocene radiometric age data were reported in Cretaceous Shimanto accretionary complex.

Hasebe et al. (1993) and Tagami et al. (1995) pointed out that the whole Cretaceous unit was cooled below 260 °C younger than 70 Ma based on the zircon fission track dating. K-Ar age was reported in this area at 55-56 Ma (Agar et al., 1989) and 67 Ma in Kii peninsula (Kurimoto, 1993). I entirely disagree with the interpretation that these episodic cooling age imply the

exhumation age (Hasebe et al., 1993; Tagami et al., 1995). These are heating ages, because paleontological data are discordant with the episodic exhumation hypothesis.

The Doganaro Formation, overlying on the northernmost portion of the Shinjogawa Group, is composed of Hauterivian to Barremian lower siliceous member and Aptian to Albian upper calcareous member. The benthic foraminifera data indicate that the lower member is deposited below the CCD, and the upper member is deposited at shallower than the CCD (Okamura, 1992). This means that the basement of the Shinjogawa Group was uplifted from Hauterivian to Albian through the CCD. The similar observation applies in the Uwajima Group, overlaying on the south of the Cenomanian Shinjogawa Group, was deposited above the CCD from Coniacian to Campanian (Taira et al., 1980; Okamura et al., 1991). This result leads to the conclusion that the Shinjogawa Group was exhumed continuously throughout Cretaceous period. The whole Cretaceous Shimanto accretionary complex was heated at latest Cretaceous to Eocene and might avoid from the Miocene thermal effect due to the pre-Miocene uplift and erosion. The thermal histry in the Shimanto accretionary complex was illustrated in Figure 23.

5.3. Thermal interaction between the oceanic crust and accretionary complex

-Estimation of fluid flow at fluid trapping stage-

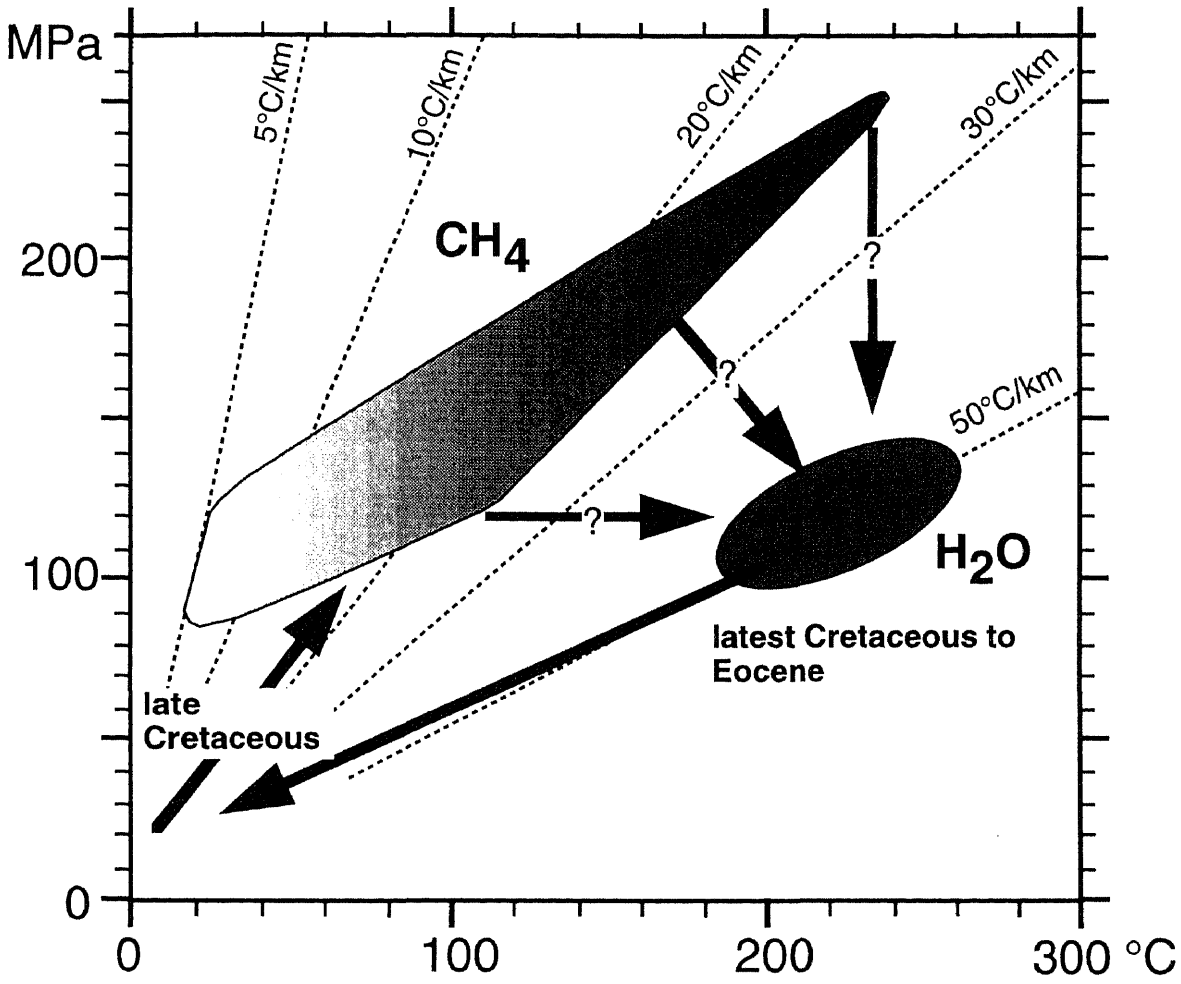

Figure 23. P-T path in the Cretaceous Shimanto accretionary complex.

To calculate the paleo-heat flow, to examine the thermal interaction between the subducting slab and accretionary prism is need. The heat flow is obtained from the geothermal gradient and thermal conductivity. Before estimating heat flow, we must pay attention to value of thermal conductivity in the accretionary prism. In the Nankai Trough, the thermal conductivity of sediment rapidly increases with depth from about 0.9 W/m°C at sea floor to about 1.4 W/ m°C at 300 m below sea floor (mbsf), and gradually increases to about 2.2 W/ m°C at 1200 mbsf (Taira et al., 1991). Which value should be used? The cover of the low thermal conductivity material varies the thermal structure. Let us make a comparison between the P-T ratios during water-rich fluid trapping of the Yokonami Melange in the Awa and Goshikigahama areas. The ratio is obtained that 201 °C/ 100 MPa in the Awa area, 199 °C/ 100 MPa in the Goshikigahama area respectively. Additionally, the ratio that is obtained from the P-T difference between the both areas are 218 °C/ 100 MPa (Fig. 24). These are very close values. The former two ratios are calculated from the thermal difference between the sea floor and deep portion. In contrast to this, the last ratio is calculated from the thermal difference between the middle portion and deep portion. If the thermal conductivity of the surface sediment is effectively low, the P-T ratio of the deeper portion becomes lower. Nevertheless, the P-T ratio of the deeper portion is nearly equal or higher than the former P-T ratio. To sum up, the low thermal conductivity zone above 300 mbsf is negligible for estimation of the heat flow.

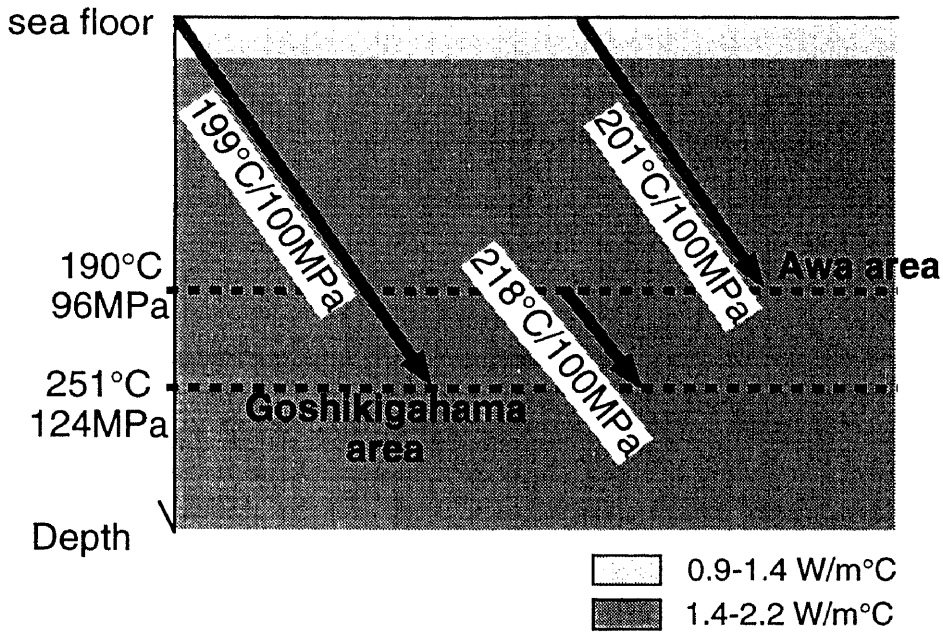

Figure 24. Distribution of the thermal conductivity in the sediment and P-T ratio.

I presume the thermal conductivity of 2.2 W/m°C, that is the value of the lowest sediment in the Nankai Trough (Taira et al., 1991). Consequently, the heat flows during water-rich fluid trapping are estimated from 95 (+70/-20) to 120 (+110/-40) mW/ m^2 in the northern thermal block. Additionally to this, much higher values are obtained in the southern coastal thermal block as over 200 mW/ m^2. The heat flows in all the formations are higher than the normal trench at present, and the heat flow increases to the south. The heat flow during methane-rich fluid trapping in the northern thermal block is 11-53 mW/ m^2.

The heat flow of the subducting oceanic crust can be made rough estimate from the age of the plate (Parsons and Sclater, 1977). The age difference between the limestone above the basalt block and black shale matrix within the Yokonami Melange is 60-70 Ma (Taira et al., 1988). If the basalt was mid ocean ridge origin, this is the age of the subducted plate and the heat flow was 57-61 mW/ m^2. Owing to ocean island origin basalt (Ishizuka, unpublished data), this age is younger than the true age of the plate. Therefore, the heat flow might be lower than this value. This heat flow is equal to or higher than the heat flow during methane-rich fluid trapping as mentioned just abpve. This indicates that the thermal effect from the subducting plate is definitively for heat flow in the accretionary prism, to say nothing of the ridge or young plate subduction.

The change of the P-T condition in the northern thermal block with

evolution of the heat flow is shown in Figure 25 that compares heat flow with depth. This illustrates that the each fluid of methane and water was trapped at the entirely differential stage of P-T condition, and the geothermal gradient changed largely.

5.4. Fluid migration within the accretionary prism

In this section, I will shift the emphasis away from the P-T framework to the detail relation between the fluid flow activity and P-T condition. The each fluid of methane and water was migrated within the accretionary prism separately at differential heating stages for each other. It seems that the mode of fluid flow differs in the heating mode. I will present the some example of fluid migration.

The rimward increase trend of homogenization temperature of the methane-rich fluid inclusions from -110 °C to -100 °C within the quartz grain (Fig. 19b) indicates the P-T change during quartz growing. This change corresponds the drop in pressure of 20-40 MPa, and reasonably supports either slow exhumation or quick fluid expulsion. In case of slow exhumation, the qurtz grains might be closely compacted. This grain might be better deposited under quick fluid expulsion, because this crystal has many of defect, namely, fluid inclusion (Fig. 19a).

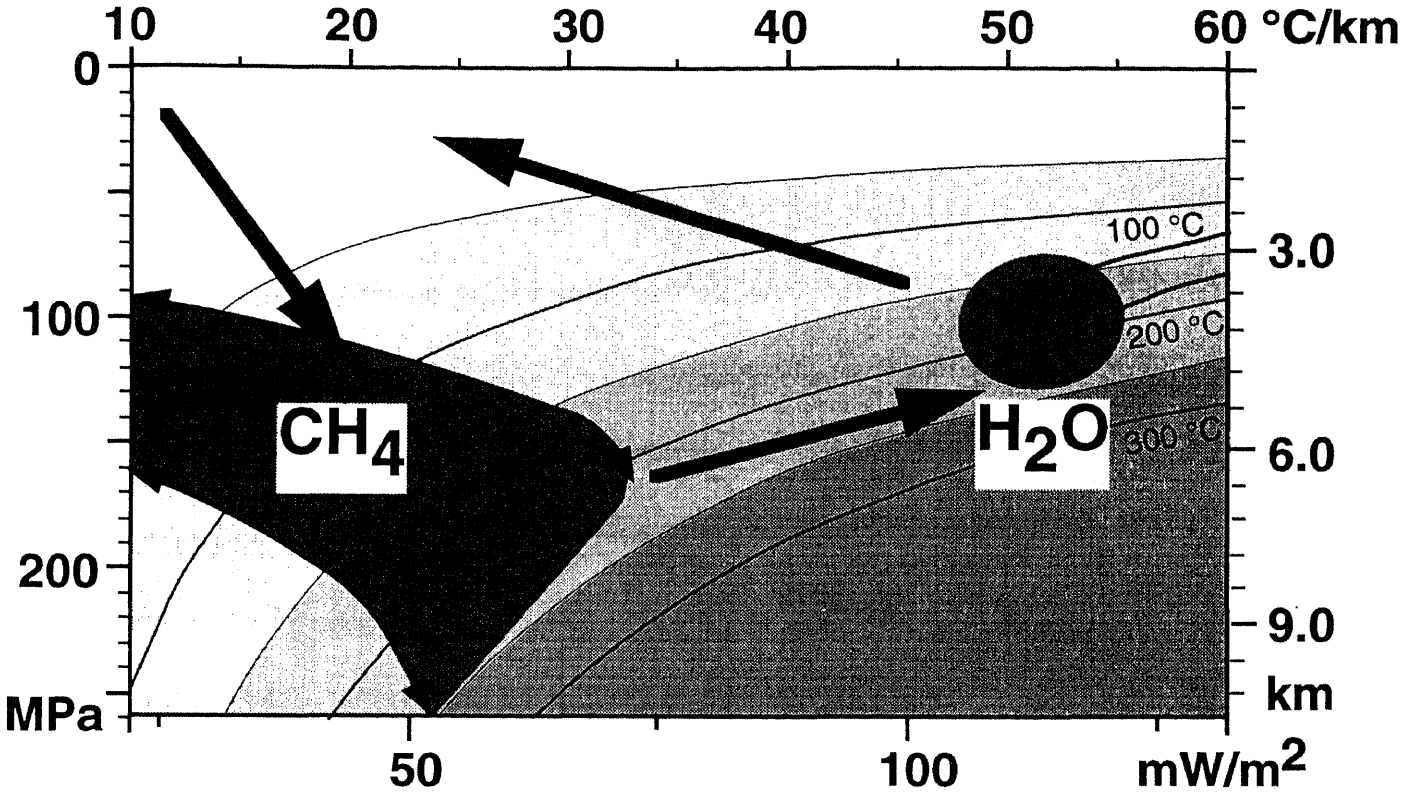

Figure 25 P-T evolution with increasing of the geothermal gradient.

The similar qurtz grain was reported in the Kodiak accretionary complex (Vrolijk, 1987; Vrolijk et al., 1988). He concluded that the warm fluid was migrated throughout the tectonic melange formation. However, the P-T difference between the melange and surrounding strata was not found in this Shimanto accretionary complex, and thus quartz grain is quite rare. The migration of methane-rich fluid was much weaker than water-rich fluid.

The homogenization temperature of water-rich fluid inclusion in the Nonokawa Formation is close to the maximum temperature by the Rm. The paleo-geothermal gradient at that time is too high to estimate by the method of this study, however, was the geothermal gradient extremely high really? The maximum P-T condition of the fluid of the Nonokawa Formation in the northern and southern areas are not plotted on the any line of the geothermal gradient. This implies that the rock did not reach thermal equilibrium state, and warm fluid was migrated throughout the Nonokawa Formation. Additionally to this, the remarkable many of small quartz veins are observed in the Okitsu Melange which suffered much higher temperature than the surrounding strata. Thus thermal situation and the rock that has remarkable many of small quartz veins is not found in the northern thermal block. It seems that the strong fluid migration in the southern coastal thermal block especially in the Okitsu Melange than the northern thermal block supplied the thermal non-equilibrium state and high temperature to the rock.

The heat flow during water-rich fluid trapping increased to trenchward

and reached over 200 mW/m^2 in the Okitsu Melange. The similar trend and high heat flow in the toe of the accretionary prism over 150 mW/m^2 is reported in the present Nankai Trough (Yamano et al., 1983; Ashi and Taira, 1993). This is explained by the hot Shikoku basin subduction and locally fluid expulsion. Such high value and trend of heat flow should be common in the case of hot plate subduction beneath an accretionary prism. The heat flow distribution in this area records the thermal structure of the accretionary prism at the highest thermal stage.

5.5. P-T condition of the melange formation

In view of obtained P-T condition, let us then consider the burial depth of the melange formation. A large number of studies have been made on the formation mechanism of the melange, and it was expected that melange was formed in the deeper portion of the accretionary prism owing to the highly sheared lithofacies, though,wever, little is known the P-T condition of the melange formation. Several articles have been devoted to the study of metamorphic grade of the exotic basalt block within the melange (Cowan, 1974; Toriumi and Teruya, 1988), however it is impossible to compare the metamorphic grade between the melange and surrounding strata. Moreover, there is the possibility that the basalt block was metamorphosed before

accretion by the Ocean-floor metamorphism (Miyashiro et al., 1971; Ishizuka, 1989).

The triaxial complession test implies that the sandstone from the melange is broken brittle under higher cofining pressure of over 150 MPa than the surrounding strata (Hada, 1988). This means, however, the sandstone from the melange was not always buried deeper than the surrounding strata because of the cataclisis. The web structure (Byrne, 1984) that is charactrized by irregular network vein of the extreme reduced grain caused by cataclasis and shearing is well developed within the sandstone. The sandstone from the melange might suffered strain hardening effectively by thus deformation (Aydin and Johnson, 1983; Hada, 1988). To sum up, there is no definite evidence that the melange was formed deeper than the other strata.

As we noted, it is not found difference of the P-T condition between the melange and surrounding strata by this study. The Yokonami Melange and surrounding strata was buried less than 6-10 km together. Additionally, the Tei area where is the eastern extension of the Yokonami Melange has the value of Rm of 1.2% (Ohmori et al., 1994), is the lowest rank of the value in the Chichibu and Shimanto accretionary complex. Though the vitrinite suffered thermal overprint, this low Rm indicates the maximum temperature of the Yokonami Melange. The Yokonami Melange might be formed at equality depth with the surrounding strata.

5.6. Exhumation tectonics of the post-peak heating

The southward increase trend of the Rmax might form by the block uplift tectonics. This point of tectonics is controversial. Awan and Kimura (1995) regarded the fault between thermal blocks as the out-of-sequence thrust. Ohmori et al. (1997) compared the block uplift tectonics to the mega-thrust activity in the present Nankai Trough. Additionally, Hibbard et al. (1992) concluded that the macro scale deformation, associated with the Muroto flexure, was occurred by the subduction of the active Shikoku basin spreading ridge and related seamounts. However, southward increaese of block uplift tectonics happened regionally, because similar southward increase trend of the thermal structure is known from the Kii Peninsula to Kyushu.

It seems that the block uplift is the common tectonics at the last stage of the accretion; however, we should also consider another locally factor, because the uplift patterns of the thermal blocks vary area to area. For example, the southern inland thermal block in the study area has northward uplift trend as mentioned before. Moreover, the strike of the thermal structure in eastern Shikoku matches the geologic structure (Mori and Taguchi, 1988; Ohmori et al., 1994) in contrast to this area, as will be mentioned in detail later. The thermal structure breaks clearly at the ATL in eastern Shikoku and middle Kyushu areas (Aihara, 1989; Murata, 1996) as opposed to this area.

The detailed thermal structural analysis may help consider the uplift process of the thermal block. I will discuss about this tectonics from the detailed quantitative uplift pattern in only the northern thermal block, because it is hard to estimate the paleo-geothermal gradient of the other thermal blocks as mentioned above.

The detailed uplift pattern of the northern thermal block around the Yokonami Peninsula is demonstrated in Figure 26, in which the value of the uplift quantity of the sampling point is plotted. The strike of iso-uplift is northeast, crossing the strike of the Shinjogawa and Taisho Groups of east-northeast trend. The block might uplift by the northeast trending fault after the accretionary complex formation.

Some of the northeast trending faults, crosscutting the Chichibu and Shimanto accretionary complexes are reported in Shikoku such as Kaminirogawa-Akuigawa and Tanono fault (Iguma and Ichikawa, 1978; Murata, 1988). These fault activities are interpreted to occur in association with clockwise rotation of Southwest Japan at middle Miocene (Yanai, 1988; Kano et al., 1990; Murata, 1990). It is possible that the thermal blocks had uplifted simultaneously.

In conclusion, the Chichibu to Shimanto accretionary complexes uplifted block by block with the effect of the regional deformation throughout southwest Japan. The fault that made the block uplift acted in the area of the forearc basin to shelf slope within the arc-trench system, because the northern

thermal block includes the forearc basin and shelf-slope sediments.

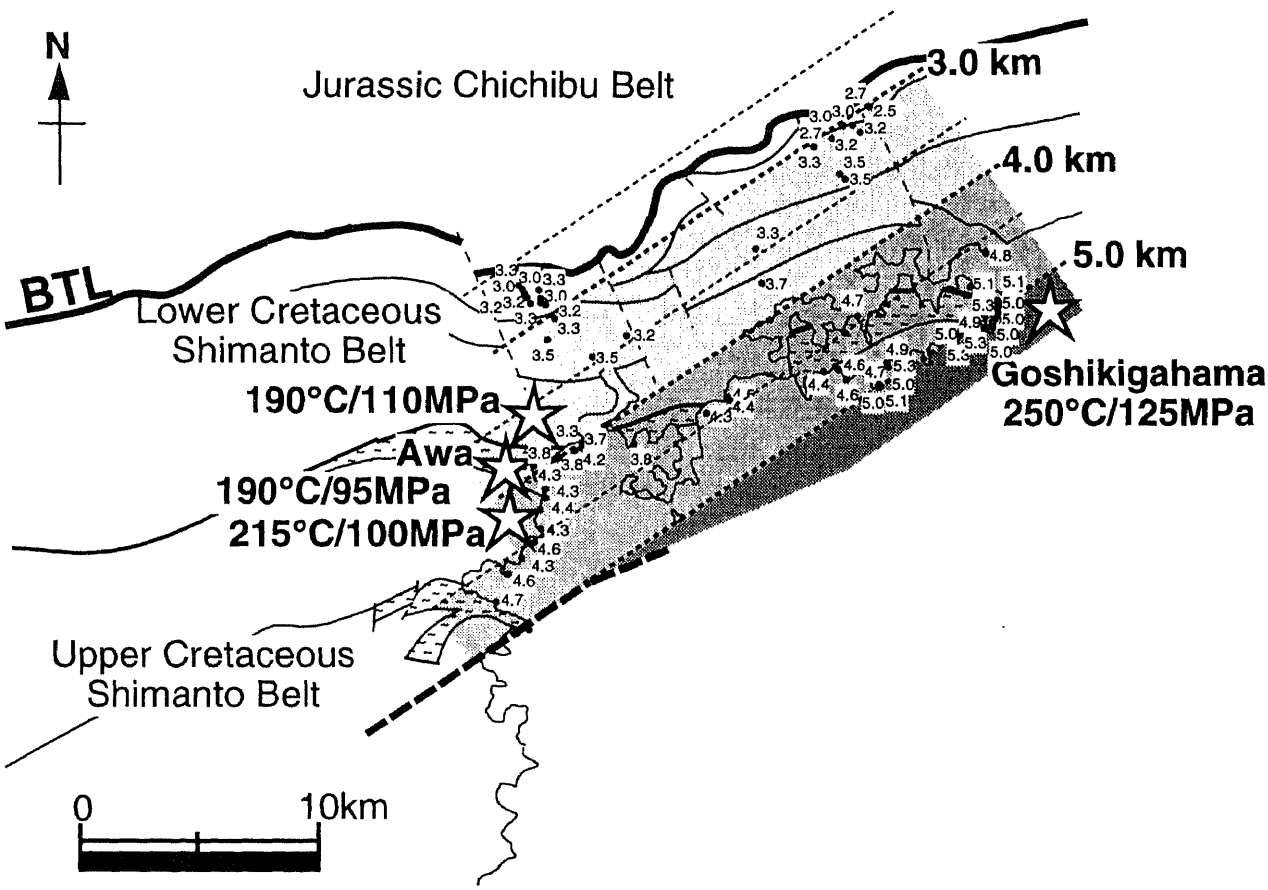

Figure 26. Detailed uplift quantity around the Yokonami Melange.

Chapter 6

CONCLUSIONS

The thermal evolution is summayed as follows. At first, the rock was buried ~10 km under the geothermal gradient of ~24 °C/km, and then the rock reached the peak temperature of 190 to 270 °C under high geothermal gradient from 50 °C/km to 90~ °C/km after the exhumation to 3-5 km in depth. In both stage, no P-T difference was found between the melange and surrounding strata except for the Okitsu Melange.

The change of the geothermal gradient corresponds to the evolution of the thermal condition of the slab, changes with age. At the later stage, the independent thermal structure from the geologic structure was formed by the thermal overprint.

The migration of the water-rich fluid transfers the heat flow to the toe of the accretionary prism. At the peak heating, the heat flow reached ~200 mW/m^2 in the Okitsu Melange that was formed concurrently with the Kula-Pacific ridge subduction at the latest Cretaceous to Eocene.

The complex was exhumed block by block after the peak heating. The southward increase trend of the thermal structure was formed by this event. The block uplift was occurred by the northwest trending fault. This fault may have occured simultaneously with the regional deformation in the southwest Japan at middle Miocene.

The metamorphism in the accretionary complex is controlled by the thermal condition of the slab even cold plate subduction to say nothing of the ridge subduction.

ACKNOWLEDGMENTS

I thank Professor Yujiro Ogawa of University of Tsukuba for reading the entire text in its original form and making helpful suggestions throughout the work. Professor Shigeho Sueno, Professor Yoshimichi Kajiwara, Dr. Mamoru Enjoji and Dr. Ken-ichiro Hisada read and criticized the manuscript. Professor Makoto Okamura of Kochi University furnished helpful comment. The vitrinite reflectance and fourier-transform infrared microspectroscopic analysis at Kyushu University was greatly assisted by Professor Atsuo Aihara and Professor Tatsushi Murae. Dr. Mamoru Enjoji of University of Tsukuba provided guidance for fluid inclusion analysis. My classmates and other students provided me the intellectual stimulation.

REFERENCES

Agar, S. M., Cliff, I. R., and Rex, D. C., 1989. Accretion and uplift in the Shimanto Belt, SW Japan. Journal of the Geological Society, 146: 893-896.

Aihara, A., 1989. Paleogeothermal influence on organic metamorphism in the neotectonics of the Japanese Islands. Tectonophysics, 159: 291-305.

Aihara, A., Chijiwa, K. and Aizawa, J., 1987. Preliminary geological study on optical anisotropy of coaly organic matter in sediments of late diagenetic (middle catagenetic) to low metamorphic stage. Memoirs Fac. Sci., Kyushu Univ., 27: 119-129.

Ashi, J., and Taira, A., 1993. Thermal structure of the Nankai accretionary prism as inferred from the distribution of gas hydrate BSRs. in Underwood, M. B., ed., Thermal evolution of the Tertiary Shimanto Belt, southwest Japan: An example of ridge-trench interaction. Geological Society of America Special Paper, 273: 137-149.

Awan, M. A. and Kimura, K., 1996. Thermal structure and uplift of the Cretaceous Shimanto Belt, Kii peninsula, southwest Japan. Island Arc, 5: 69-88.

Aydin, A. and A. M. Johnson, 1983. Analysis of faulting in porous sandstone. Journal of Structural Geology, 5: 19-31.

Barker, C. E., 1988. Geothermics of petroleum systems. Implications of the stabilization of kerogen thermal maturation after a geologically brief heating duration at peak temperature. in Magoon, L., ed., Petroleum systems of the United States: U.S. Geological Survey Bulletin 1870: 26-29.

Brown, E. P., 1989. FLINCOR: A microcomputer program for the reduction and investigation of fluid-inclusion data. American Mineralogist, 74:

1390-1393.

Byrne, T., 1984. Early deformation in melange terranes in the Ghost Rocks Formation, Kodiak Islands, Alaska. in Raymond, L. A., ed., Melange: their nature, origin and significance. Geological Society of America, special paper, 198: 21-52.

Byrne, T., and DiTullio, L., 1992. Evidence for changing plate motions in southwest Japan and reconstructions of the Philippine Sea plate. Island Arc, 1: 148-165.

Chamot-Rooke and others, 1992. Tectonic context of fluid vending at the toe of the eastern Nankai accretionary prism: Evidence for a shallow detachment fault. Earth and Planetary Science letters, 109: 319-332.

Chijiwa, K., 1988. Post-Shimanto sedimentation and organic metamorphism: an example of the Miocene Kumano Group, Kii peninsula. Modern Geology, 12: 363-387.

Cowan, D. S., 1974. Deformation and metamorphism of Franciscan subduction zone complex northwest of Pacheco Pass, California. Geological Society America Bulletin, 89: 1623-1634.

Cowan, D. S., 1985. Structural styles in Mesozoic and Cenozoic melanges in western Cordillera of North America. Geological Society America Bulletin, 96: 451-462.

DiTullio, L., Laughland, M. M., and Byrne, T., 1993. Thermal maturity and constraints on deformation from illite crystallinity and vitrinite reflectance in shallow levels of an accretionary prism. Eocene-Oligocene Shimanto Belt, southwest Japan. in Underwood, M. B., ed., Thermal evolution of the Tertiary Shimanto Belt, southwest Japan: An example of ridge-trench interaction. Geological Society of America Special Paper, 273: 63-82.

Dumitru, T. A., 1991. Effects of subduction parameter on geothermal

gradients in Forearcs, with an application to Franciscan subduction in California. Journal of Geophysical Research, 96: 621-641.

Engebretson, D. C., Cox, A., and Gordon, R. G., 1985. Relative motions between oceanic and continental plates in the Pacific basin. Geological Society of America Special Paper, 206: 59

Hada, S., 1988. Physical and mechanical properties of sedimentary rocks in the Cretaceous Shimanto Belt. Modern Geology, 12: 341-359.

Hasebe, N., Tagami, T., and Nishimura, N., 1993. Evolution of the Shimanto accretionary complex. A fission-track thermochronologic study. in Underwood, M. B., ed., Thermal evolution of the Tertiary Shimanto Belt, southwest Japan: An example of ridge-trench interaction. Geological Society of America Special Paper, 273: 121-136.

Hibbard, J. P., and Karig, D., 1990. An alternative plate model for the early Miocene evolution of the SW Japan margin. Geology, 18: 170-174.

Hibbard, J. P., Karig, D., and Taira, A., 1992. Anomalous structural evolution of the Shimanto accretionary prism at Murotomisaki, Shikoku island, Japan. Island Arc, 1: 133-147.

Hibbard, J. P., Laughland, M. M., Kang, S. M., and Karig, D., 1993. The thermal imprint of the ridge subduction on the upper structural levels of an accretionary prism, southwest Japan. in Underwood, M. B., ed., Thermal evolution of the Tertiary Shimanto Belt, southwest Japan: An example of ridge-trench interaction. Geological Society of America Special Paper, 273: 83-101.

Hsu, J. K., 1968. Principles of melange and their bearing on the Franciscan-Knoxville paradox. geological Society of America Bulletin, 79: 1063-1074.

Kano, K., Nakaji, M. and Takeuchi, S., 1991. Asymmetrical melange fabrics as possible indicators of the convergent direction of plates: a case study

from the Shimanto Belt of the Akaishi Mountains, central Japan. Tectonophysics, 185: 375-388.

Kiminami, K. and Miyashita, S., 1992. Occurrence and geochemistry of greenstones from the Makimine Formation in the Upper Cretaceous Shimanto Supergroup in Kyushu, Japan. Journal of Geological Society of Japan, 98: 391-400.

Kiminami, K., Kashiwagi. N. and Miyashita, S., 1992. Occurrence and significance of in-situ greenstones from the Mugi Formation in the Upper Cretaceous Shimanto Supergroup, eastern Shikoku, Japan. Journal of Geological Society of Japan, 98: 867-883.

Kimura G. and Mukai, A., 1991. Underplated units in an accretionary complex: Melange of the Shimanto belt of eastern Shikoku, southwest Japan. Tectonics, 10: 31-50.

Kimura, K., 1985. Stratigraphical and sedimentological facies of the Tertiary Shimizu and Misaki Formations in southwestern part of Shikoku. Jour. Geol. Soc. Japan, 91: 815-831 (in Japanese with English abstract).

Kumon, F., 1992. Albitization of detrital plagioclase in the Cretaceous sandstones from the Shimanto Belt in the eastern Shikoku, southwest Japan. in Kiminami, K., et al., eds., Composition and origin of clastic rocks from mobile belts -examples from the Japanese island. Memoirs Geol. Soc. Japan, 38: 281-291 (in Japanese with English abstract).

Kurimoto, C., 1982. Chichibu system in the area southwest of Koyasan, Wakayama prefecture: upper Cretaceous Hanazono Formation. Jour. Geol. Soc. Japan, 88: 901-914 (in Japanese with English abstract).

Laughland, M. M., and Underwood, M. B., 1993. Vitrinite reflectance and estimates of paleotemperature within the Upper Shimanto Group, Muroto Peninsula, Shikoku, Japan. in Underwood, M. B., ed., Thermal evolution of the Tertiary Shimanto Belt, southwest Japan. An example of

ridge-trench interaction. Geological Society of America Special Paper, 273: 103-114.

Maruyama, S., and Seno, T., 1986. Orogeny and relative plate motions: example of the Japanese islands. Tectonophysics, 127: 305-329.

Mecker, K. and others, 1988. Costa Rica Rift 3. Site 504: Costa Rica Rift. Proceedings of the Ocean Drilling Program, Part A-Initial Reports, 111: 35-251.

Moor, J. C. and Wheeler, R. L., 1978. Structural fabric of a melange, Kodiak island, Alaska. American Journal of Science, 278: 739-765.

Moor, J. C. and others, 1995. Abnormal fluid pressures and fault-zone dilation in the Barbados accretionary prism: Evidence from logging while drilling. Geology, 23: 605-608.

Mori, K., and Taguchi, K., 1988. Examination of the low-grade metamorphism in the Shimanto Belt by vitrinite reflectance. Modern geology, 12: 325-339.

Morino, Y., 1993. Depositinal environments of the lower Cretaceous Torinosu type limestone in the Monobe area, Kochi Prefecture. Journal of Geological Society of Japan, 99: 173-183.

Murae, T., Microphotometric and organic geochemical studies on alteration of woody tissues of fossilized plant during diagenetic and burial-metamorphic processes. Science Report, Kyushu Univ. 18: 25-35 (in Japanese with English abstract).

Murata, A., 1989. Lateral change of horizontal displacement along the Kaminirogawa-Akuigawa fault in eastern Shikoku. Journal of Geological Society of Japan, 94: 689-695 (in Japanese with English abstract).

Murata, A., 1990. Displacement distribution along the Kaminirogawa-Akuigawa fault and dislocation model. Journal of Geolography of Japan, 99: 370-381(in Japanese with English abstract).

Murata, A., 1995. Thermal structure of hanging wall of the Nobeoka thrust using illite crystallinity in eastern Kyushu. Abstracts of 102nd annual meeting of Geological Society of Japan: 218 (in Japanese).

Ogawa, Y., and Taniguchi, H., 1989. Origin and emplacement of basaltic rocks in the accretionary complexes in SW Japan: Ofioliti, 14: 177-193.

Ohmori, K., 1994. Thermal structure and uplift history of the northern Shimanto Belt, Shikoku -Vitrinite reflectance study-. Master thesis, Department of Geology, Univ. Tokyo.

Ohmori, K., Taira, A., Tokuyama, H., Sakaguchi, A., Okamura, M. and Aihara, A., 1997. The paleo-thermal structure of the Shimanto accretionary prism, Shikoku, Japan -vitrinite reflectance study-. Geology (Submitting).

Okamura, M., 1992. Cretaceous Radiolalia from Shikoku, Japan (Part 1). Memoirs Fac. Science, Kochi Univ. 13:21-164.

Okamura, M. and Matsugi, H., 1986. Cretaceous radiolarians from the time-equivalent formations of arc-trench system, Shikoku. News of Osaka Micropaleont. Spec. 7: 117-129.

Okamura, M., Umemura, H. and Yasuda, H., 1991. Lithofacies and deformation of the Shimanto Belt, southwestern part of Shikoku. Excursion guidebook, the 98th annual meeting of the Geological Soc. Japan: 85-120 (in Japanese).

Okano, H., 1992. Thermal history of accretionary prism in Ashizuri district, southwest Japan. graduate thesis, Department of Geology, Univ. Kochi (in Japanese with English abstract).

Parsons, B. and Sclater, J. G., 1977. An analysis of the variation of ocean floor with age. Journal of Geophysical Research, 82: 803-827.

Pironon, J., Sawatzki, J. and Dubessy, J., 1991. NIR FT-Raman microspectroscopy of fluid inclusions: comparisons with VIS Raman and

FT-IR microspectroscopies. Geochimica et Cosmochimica Acta, 55: 3885-3891.

Potter, II, R. W., Clynne, M. A. and Brown, D. L., 1978. Freezing point depression of aqueous sodium chloride solutions. Economic Geology, 73: 284-285.

Sakaguchi, A., Ohmori, K., Yamamoto, H., Aihara, A., and Okamura, M., 1992. Paleo-geothermal structure of the Cretaceous Shimanto Belt analyzed by vitrinite reflectance, central Shikoku, southwest Japan. Research Report of Kochi University, 41: 29-48 (in Japanese with English abstract).

Sakaguchi, A., Okamura, M. and Aihara, A., 1994. Thermal structure of the Shimanto Belt and a ridge subduction. Earth Monthly, 16:468-472 (in Japanese).

Sakaguchi, A., 1996. High geothermal gradient with ridge subduction beneath Cretaceous Shimanto accretionary prism, southwest Japan. Geology, 24: 795-798.

Sakamoto, T., Ogawa, Y., and Nakada, S., 1993. Origin of the greenstones in the Setogawa accretionary complex and their tectonic significance: Journal of the Geological Society of Japan, 99: 9-28 (in Japanese with English abstract).

Sample, J. C. and Moor, J. C., 1987. Structural style and kinematics of underplated slate belts, Kodiak and adjacent islands, Alasuka. Geological Society of America Bulletin, 99: 7-20.

Sasada, M., 1989. Microthermometry of fluid inclusions in minerals from geothermal fields. Geothermal Energy, 14: 27-42 (Japanese).

Saxena, S. K. and Fei, Y., 1987. Fluids at crustal pressureand temperatures I. pure species. Contributions to Mineralogy and Petorology, 95: 370-375.

Seno, T., 1988. Tectonic evolution of the west Philippine basin. Modern

Geology, 12: 481-495.

Seno, T., and Maruyama, S., 1984. Paleogeographic reconstruction and origin of the Philippine sea. Tectonophysics, 102: 53-84.

Shepherd, T. J., 1981. Temperature programmable heating-freezing stage for microthermometric analysis of fluid inclusions. Economic Geology.

Shepherd, T. J., Rankin, A., and Alderton, D. H., 1985. A practical guide to fluid inclusion studies: Glasgow, Blackie and Son: 239.

Shi, Y., and Wang, C., 1985. High pore pressure generation in sediments in front of the Barbados Ridge complex: Geophysical Research Letters, 12: 773-776.

Shibata, K. and Nozawa, T., 1968. K-Ar ages of granitic rocks of Ashizuri-misaki, Takatsukiyama and Omogo, Shikoku, Japan. Bull. Surv. Japan, 19: 11-16.

Suzuki, S., Oda, Y. and Nambu, M., 1982. Thermal alteration of vitrinite in the Miocene sediments of Kishu mine area, Kii peninsula, Japan. Jour. Soc. mining Geol. Japan, 32: 55-65 (in Japanese with English abstract).

Tagami, T., Hasebe, N. and Shimada, C., 1995. Episodic exhumation of accretionary complex: Fission-track thermochronologic evidence from the Shimanto Belt and its vicinities, southwest Japan. Island Arc, 4: 209-230.

Taira, A., Tashiro, M., Okamura, M. and Katto, J., 1980. The geology of the Shimanto Belt in Kochi Prefecture, Shikoku, Japan, in Taira, A., and Tashiro, M., eds., Geology and paleontology of the Shimanto Belt: Kochi, Japan, Rinyakoseikai Press: 179-214 (in Japanese with English abstract).

Taira, A., Katto, J., Tashiro, M., Okamura, M., and Kodama, K., 1988. The Shimanto Belt in Shikoku, Japan -Evolution of Cretaceous to Miocene accretionary prism: Modern Geology, 12: 5-46.

Taira, A., Hill, I., Fish, J., and others, 1991. Proceedings of the Ocean Drilling Program, Initial Reports, 131: College Station, Texas, Ocean Drilling Program: 71-269.

Takahashi, M., (1980). Voluminous felsic magma activity and upper crust formation in the mobile zone. Earth Monthly, 2: 837-845 (in Japanese).

Tanabe, H. and Kano, K., 1996. Illite crystallinity study of the Cretaceous Shimanto Belt in the Akaishi Mountains, eastern Southwest Japan. Island Arc, 5: 56-68.

Tokunaga, T., 1992. Duplexing and intraprism deformation of the Paleogene Shimanto super Group in western Shikoku, southwest Japan. Tectonics, 11:1168-1179.

Toriumi, M. and Teruya, J., 1988. Tectono-metamorphism of the Shimanto Belt. Modern Geology, 12: 303-324.

Underwood, M. B., Laughland, M. M., Byrne, T., Hibbard, J. P., and DiTullio, L., 1992. Thermal evolution of the Tertiary Shimanto Belt, Muroto Peninsula, Shikoku, Japan. Island Arc, 1: 116-132.

Underwood, M. B., Hibbard, J. P., and DiTullio, L., 1993. Geologic summary and conceptual framework for the study of thermal maturity within the Eocene-Miocene Shimanto Belt, Shikoku, Japan, in Underwood, M. B., ed., Thermal evolution of the Tertiary Shimanto Belt, southwest Japan: An example of ridge-trench interaction. Geological Society of America Special Paper 273: 1-24.

Yamano, M., Honda, S., and Uyeda, S., 1984. Nankai Trough: A hot trench?. Marine Geophysical Researches, 6: 187-203.

Yanai, S. 1986. Megakink Bands and Miocene Regional Stress Field in Outer Southwestern Japan. Scientific Papers of the College of Arts and Sciences, the University of Tokyo, 36: 55-79.